Y-CRACKING IN CONTINUOUSLY REINFORCED CONCRETE PAVEMENTS

by

AMIR FARID MOMENI

B.A., Ferdowsi University of Mashhad, 2010

A THESIS

Submitted in partial fulfillment of the requirements for the degree

MASTER OF SCIENCE

Department of Civil Engineering
College of Engineering

KANSAS STATE UNIVERSITY
Manhattan, Kansas

Spring 2013

Approved by:

Major Professor
Dr Kyle A. Riding P.E

Copyright

Abstract

When transverse cracks meander there is a high possibility for transverse cracks to meet at a point and connect to another transverse crack, creating a Y-crack. Y-cracks have been blamed for being the origin of punchouts and spallings in CRCPs. When the direction of maximum principal stress changes, it could cause a change in the crack direction, potentially forming a Y-crack. Finite Element Models (FEMs) were run to model the change in principal stress direction based on design and construction conditions. The finite element model of CRCP using typical Oklahoma CRCP pavement conditions and design was assembled. The model included the concrete pavement, asphalt concrete subbase, and soil subgrade. The effect of areas of changed friction on the direction of principal stress was simulated by considering a patch at the pavement-subbase interaction. Investigated factors related to this patch were location of patch, friction between patch and subbase, and patch size. Patches were placed at two different locations in the pavement: a patch at the corner of the pavement and a patch at the longitudinal edge between pavement ends. A change in the friction at the corner had a large effect on the stress magnitude and direction of principal stress, while a patch in the middle did not significantly change the stress state. Also, patch size had a noticeable effect on stress magnitude when the patch was at the corner. Another model was developed to understand the effect of jointed shoulder on direction of maximum principal stress. Analysis of this model showed that the stresses were not symmetric and changed along the width of the pavement. This meandering pattern shows a high potential for Y-cracking. Also, several finite element models were run to understand the effects of different shrinkage between mainline and shoulder. In order to simulate the effects of the differential drying shrinkage between the hardened mainline concrete and the newly cast shoulder, different temperature changes were applied on the mainline and shoulder.

For these models, the orientation of the maximum principal stress was not significantly changed from different amounts of temperature decreases between mainline and shoulder. Also, effect of different longitudinal steel percentages was investigated by comparing two finite element models with different steel percentage. The model with higher steel percentage (0.7%) indicated more variation in stress, potentially leading to more crack direction diverging.

Table of Contents

List of Figures

List of Tables

Chapter 1 Introduction

CRCP Behavior

A Continuously Reinforced Concrete Pavement (CRCP) is a portland cement concrete pavement made with embedded reinforcement and without joints. CRCPs were first built for experimental purposes in 1921 on the Columbia pike near Arlington, Virginia (Choi & Roger, 2005). CRCPs later became more popular and other states around the U.S started to construct sections of their pavements with CRCPs.

CRCP allows concrete to crack in order to relieve the stress from restrained moisture and temperature changes. Having small width transverse cracks at regular intervals along the length of CRCP is very normal and does not cause low serviceability or rough ride. However, wider transverse cracks are an issue and should be avoided. The problem with wider cracks is that they let incompressible material and water enter the pavement structure and cause spalling and pumping of subbase materials. Crack spacing and crack width are related to each other. Longitudinal reinforcements are used in CRCPs to keep the cracks tight and control crack spacing in transverse cracks.

Problem Description

One of the common problems in CRCPs is Y-cracking. Generally, when small spaced transverse cracks meander, it is very possible for these transverse cracks to meet each other at a point and form an area connected to another transverse crack, forming a Y-crack. Y-cracks have been thought to be a significant problem in CRCPs because it has been thought to lead to deterioration of the pavement. CRCPs are generally designed for heavy traffic roads and are exposed to heavy loads during their service life. When Y-cracks are loaded because of

continuous traffic, it is thought that they could lead to punchouts and spallings. Punchouts in CRCPs are usually considered as a detached block of CRCP surrounded by two closely-spaced transverse cracks, a short longitudinal crack, and the edge of pavement. Spallings are sections of concrete at the surface of the transverse cracks and joints that break off. Since Y-cracks in CRCPs are thought to lead to punchouts and spallings, Y-cracks should be prevented.

Research Objective

In this project, the Abaqus CAE software package was used to model pavement structures in Oklahoma. Several models were run to understand the effects of pavement design, materials, and construction parameters on Y-cracking. As mentioned before, Y-cracking happens when transverse cracks meander and meet each other at a point. The direction of cracking usually occurs perpendicular to direction of maximum principal stress. A change in direction of principal stress shows a change in direction of cracking, potentially Y-cracking. Finite Element Models (FEMs) were used to understand the change in principal stress direction based on different pavement geometries and properties. Any change in principal stress direction due to a change in geometry or property of pavement structure can be considered a high potential cause of Y-cracking.

Research Scope

The pavement structure was assembled in Abaqus CAE using three different material layers: concrete pavement, subbase and subgrade. All values for geometry and properties of the CRCP models were based on typical values of CRCP in Oklahoma. Mechanical and thermal properties were defined for materials in all three layers. Interactions between layers were defined

and layers were assembled on each other. Boundary conditions for the pavement structure were defined for the bottom and sides of the subgrade and the gravity load was applied to the whole model. A temperature decrease of 50^{o} F was applied to the concrete pavement, while the temperature for the subbase and subgrade was kept constant. This temperature loading was used as a simulation for the cumulative drying shrinkage and temperature change of the pavement.

The effect of subbase non-uniformity on direction of principal stress was experimented by adding a patch to the pavement or in the other words having a changed friction area in the pavement. The effect of these patches on change in direction of principal stress was studied by varying the patch location in the pavement, patch size and friction coefficient of interaction between patch and subbase.

The impact of having jointed shoulder in the pavement on Y-cracking was simulated by adding a jointed shoulder to the right side of the main line in the basic finite element model. All the other parameters were as the same as the basic model. This model was run to understand the effect of jointed shoulder in CRCP on direction of principal stress along the width of the pavement.

Several finite element models were run to see the effect of different shrinkage between mainline and shoulder. In order to simulate the effects of the differential drying shrinkage between the hardened mainline concrete and the newly cast shoulder, different temperature changes were applied on the mainline and shoulder. Direction of principal stresses was calculated along the width of the pavement in the middle of the pavement between two ends and at the transverse edge of the pavement to understand the possibility of change in cracking direction.

The other factor experimented in order to understand its impact on direction of principal stress was longitudinal steel percentage. Two models with different longitudinal steel percentage were compared. Diameter of longitudinal steel bars for both models of 0.6 and 0.7 percent longitudinal steel was 0.75 in.

Organization of Thesis

This thesis is organized in 5 chapters. Following chapter 1, works done on CRCPs in the past are discussed in chapter 2 - Literature Review. Chapter 3 includes methods used for the finite element modeling. In chapter 4, results of finite element models are presented. Lastly, in chapter 5, conclusion and recommendation are made.

Chapter 2 Literature Review

Continuously Reinforced Concrete Pavement

A Continuously Reinforced Concrete Pavement (CRCP) is a type of portland cement concrete (PCC) pavement without transverse joints. CRCP may continue thousands of feet without transverse joints, except for construction joints. Anchorage is used at the end of pavement section in order to limit length changes due to thermal and moisture changes in the pavement (Shiraz, Stephanos, Gagnon, & Zollinger, 1998). CRCPs are allowed to crack at regular intervals to relieve the stresses associated with shrinkage. The environmental circumstances at the time of building, steel percentage, and concrete strength control the cracking pattern. Longitudinal reinforcements are used in CRCPs to control transverse crack spacing and width. A continuous longitudinal reinforcement produces random transverse cracks in the concrete pavement and relieves some of the shrinkage stresses (Choi & Roger, 2005). As steel bars several miles long cannot be manufactured or transported, steel bars are spliced to give continuous reinforcement. Since volume changes due to hydration and climate in concrete are restrained by reinforcement and the pavement base, transverse cracks progress at regular intervals. Reinforcing concrete pavements results in closer spaced cracks and smaller crack widths, therefore, a better ride (Kohler & Roesler, 2004). Longitudinal joints are used to release concrete transverse stresses or when pavement construction should be in more than one pass. When good methods for design and construction are adopted, CRCPs are one of a few pavement types that need very little maintenance (Shiraz, Stephanos, Gagnon, & Zollinger, 1998). Compared to other form of pavements, CRCPs have shown outstanding long term performance with a significant decrease in both annual and life-cycle costs (The Transtec Group, Inc., 2004).

Problem Description

Narrow width cracks are not considered a problem in CRCPs since a crack with small width allows efficient load transfer and prevents incompressibles,from entering (Kohler & Roesler, 2006). However, when transverse cracks meander, there is a high possibility for transverse cracks to meet each other at a point and form an area which is connected to a transverse crack, forming a Y-crack (see Figure 2.3). Y-cracks have been thought to cause punchouts and spalling distresses in concrete pavements.

Punchouts

Punchouts are a type of permanent distress usually created close to the edge of the concrete pavements resulting from continuous traffic load (Kohler & Roesler, 2004). Punchouts in CRCPs are usually defined as a block of CRCP surrounded by two closely-spaced transverse cracks, a short longitudinal crack, and the edge of pavement. Closely-spaced transverse cracks become wider due to climate, concrete shrinkage, and lack of aggregate interlock. Transverse flexural stresses developed by traffic load and curling and warping of the pavement slab can cause a longitudinal crack usually 0.6 to 1.5 m from the edge of pavement. These transverse and longitudinal cracks may ultimately cause a punchout. Space between cracks, pavement depth, weak foundation support and high traffic loading are influential factors for punchout distress (Shiraz, Stephanos, Gagnon, & Zollinger, 1998). Weak foundation support can be created by base material pumping and decrease support stiffness which further increase the intensity of the punchout depression. Factors such as use of a sufficient amount of reinforcement, use of non-erodible base materials, use of aggregates with low coefficient of thermal expansion (CTE), use of bond breaker layer, adopting an appropriate curing method, and using a suitable concrete mixture for the given environmental conditions can reduce punchouts (ERES Consultants, Inc.,

2001). Punchout distress has been considered the most serious performance problem for CRCPs and they can even cause corrosion of the concrete/steel interface at the crack (Kohler & Roesler, 2006).

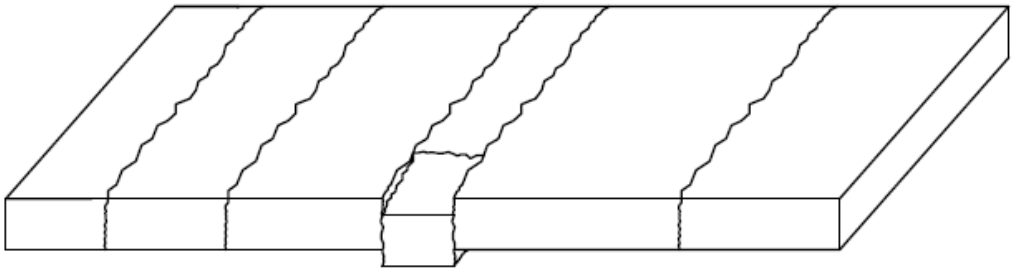

Figure 2.1 Punchout between two closely spaced transverse cracks in CRCP After (Kohler & Roesler, 2006)

Spalling

Another type of distress associated with CRCPs is spalling. Spalling is generally the breakup of concrete at the surface of pavement along cracks and joints causing reduced cross section and weak load transfer (ERES Consultants, Inc., 2001). Break ups of concrete on one side or both sides of a crack in CRCP are considered spalling. Categorization of spalls is mostly based on their depth into the pavement; a spall is assumed deep when its depth is larger than 2.5 cm (1 in.). Experiments done in the past indicated that spalling is related to crack width. Spalling increases as cracks widen. Structural flaws are generally the reason for deeper spalls, while weak horizontal planes in the surface of a slab are the reason for shallow and wide area spalls. Spalling makes the pavement appearance unpleasant which can cause drivers to think negatively about the pavement. Pavement roughness increases with an increase in spalling. This causes lower ride quality and smoothness in the pavement. Spalling decreases pavement cross section at

the joint. A thinner cross section can result in lower load transfer at joints or cracks which causes larger stresses in the pavement. Investigations showed that spalling usually happens on one side of the crack even if there are weak planes in the surface of pavement on both sides of crack. Spalls usually occur on the downstream side of the transverse cracks which is in direction of traffic. The type of coarse aggregate used in concrete slab affects severity of spalling. For example, concrete pavements with Siliceous River Gravel (SRG) as coarse aggregate have suffered more severe spalling deteriorations. This type of deterioration which was caused by using SRG as coarse aggregate occurred in Houston concrete pavements. Pavement construction practices are a primary factor in reducing spalls. An appropriate concrete mixture, good quality control, and curing method can reduce shrinkage stresses at early ages substantially. This will reduce the probability of having weak planes in the surface of pavement (Zollinger, 1994). Spalling can also develop in concrete pavements due to moisture loss at the surface of the pavement during curing time, inappropriate mixture proportions, and poor finishing methods. Excessive deflection of the pavement slab due to inadequate load transfer, traffic loading and penetrating of incompressibles into the cracks can ultimately cause spalling. Adequate steel reinforcement and use of non-erodible base material can minimize spalling. Adequate steel reinforcement helps to reduce spalling by keeping cracks tight and preventing excessively large spaced cracks (ERES Consultants, Inc., 2001).

Figure 2.2 Spalling at transverse joint in concrete pavement

History of CRCP

CRCPs were constructed for the first time for experimental purposes in 1921 on Columbia Pike near Washington, D.C. Several years later, the next CRCP was constructed near Indianapolis. The design of CRCP was added to a 1993 guide by the American Association of State Highway and Transportation Officials (AASHTO) (Choi & Roger, 2005). By the 1940s and 1950s many states started to conduct broad studies on the effects of different designs and construction elements on CRCP performance. These experimental projects occurred in Illinois and New Jersey in 1947, California in 1949, and Texas in 1951 (Kohler & Roesler, 2006). The wide use of CRCP started in the early 1960s and now more than 45,080 lane kilometers (KM) (28,000 lane miles (mi)) of CRCP exists throughout over 35 states in the United States (Choi & Roger, 2005).

Oklahoma History

The continental climate in Oklahoma creates a significant weather variation during the seasons. Since the climate variation in Oklahoma is very high, durability is an important factor in choosing the type of concrete pavement (Shiraz, Stephanos, Gagnon, & Zollinger, 1998). 1104 lane km (686 lane miles) of CRCP were built in Oklahoma since early 1970s. Approximately 75 percent of CRCPs in Oklahoma were constructed since 1986. CRCPs in Oklahoma are mostly in the eastern half of the state; however there are a few in the western half of state. The first CRCPs in Oklahoma were designed with 0.6 percent of longitudinal steel bar in the early to mid-1970s. The use of CRCPs was stopped until the mid-1980s when CRCPs were built again in the state using 0.5 percent longitudinal steel bars,In almost 1990, the percentage of longitudinal reinforcing steel was increased to 0.6 percent for CRCPs in Oklahoma. There are differences in geometry and material of base and shoulder of Oklahoma CRCPs built in different decades. As of 1996, the latest CRCP was constructed with an open graded, cement treated base and tied PCC shoulders (McGovern, Ooten, & Senkowski, 1996).

Texas History

Texas has the highest mileage of CRCPs in United States. Based on CRCPs performance results in Indiana and Illinois in the 1930s and 1940s, the first CRCP in state of Texas was constructed in 1951 in Fort Worth. All concrete pavements exposed to heavy traffic loading are CRCP type in state of Texas. Crack width, Crack spacing and stress state of reinforcement are important parameters in CRCPs which were taken into account after studies done by TxDOT over past several decades. Over the recent decades, TxDOT has implemented models which can relate CRCPs properties to each other (The Transtec Group, Inc., 2004).

Typical cracks in CRCPs

CRCPs are generally constructed to crack naturally with predictable average crack spacing. Crack spacing is dependent on the steel percentage, bond between concrete and steel, base friction and properties of concrete mix. CRCPs are typically associated with four types of crack which are: meandering, divided, cluster, and Y-cracks (see Figure 2.3). Y-cracks and cluster cracks can often cause punchouts and spallings. Cluster cracking refers to an average of five isolated cracks spaced less than 2 ft. (Kohler & Roesler, 2004). Cluster cracks can come to existence in CRCPs due to variation in subgrade support, poor concrete consolidation, short drainage, high base friction, and high ambient temperature at the time of construction (McGovern, Ooten, & Senkowski, 1996). Y-cracking is defined by a transverse crack that splits into two other cracks that spread apart. All these crack patterns, especially cluster cracking and Y-cracking can cause punchouts and spalling (Johnston & Surdahl, 2008). Steel depth and concrete shrinkage affect amount of Y-cracks and cluster cracks. As steel depth increases, Y-cracking decreases. However, cluster cracking increases with increase in depth of steel. Also, with increase in concrete shrinkage, Y-cracking decreased, while the result was vice versa for cluster cracking (Kohler & Roesler, 2004).

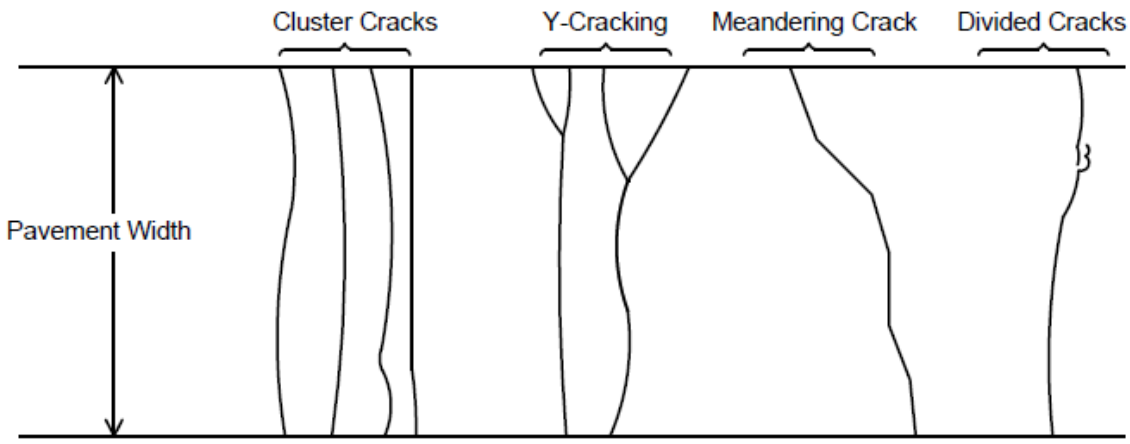

Figure 2.3 Associated types of cracks and crack patterns in CRCP
After (Kohler & Roesler, 2004)

Design of CRCP

CRCPs are generally designed as an alternative choice for roads with heavy traffic in the US and worldwide. Also, where the delays related to restoration and rehabilitation must be minimized, CRCPs can be considered as an excellent choice. Due to short maintenance cost and outstanding long term performance, CRCPs have been considered as a wise choice for heavy trafficked roads (ERES Consultants, Inc., 2001).

CRCPs are designed without transverse joints and reinforcement embedded in the concrete slab. The free-jointed concrete slab decreases maintenance costs by removing the costs for sealant materials and sealing operations (The Transtec Group, Inc., 2004). The CRCPs are allowed to crack naturally at a space about 0.9 to 2.4 m (3 to 8 ft.) with a random pattern. The cracking pattern that will follow is dependent on the environment and weather at construction time, percentage of steel and concrete strength (Shiraz, Stephanos, Gagnon, & Zollinger, 1998). Engineers passively control cracking pattern and average crack spacing by changing the percentage of longitudinal steel. Reinforcement in pavement holds transverse cracks created by

thermal and drying shrinkage tight. Addition of steel to concrete pavement creates a pavement with transverse cracks closer to each other and tighter cracks compared to Jointed Plain Concrete Pavement (JPCP). Consequently, CRCPs ride is smoother than JPC pavements (Kohler & Roesler, 2004).

In newer CRCP design standards, the type of coarse aggregate is considered an important parameter. Coarse aggregates with higher Coefficient of Thermal Expansion (CTE) lead to more distresses such as: cracks, spalling, and punchouts. For instance, concrete pavements with Siliceous River Gravel (SRG) that have a high CTE have more expansions and cracks than pavements made with limestone aggregates with a low CTE for the same reinforcement design. Using limestone led to larger crack spacing and tighter cracks than SRG in one Texas study (The Transtec Group, Inc., 2004). The parameters in coarse aggregates which may be related to tighter cracks and larger crack spacing are smaller CTE, larger strain capacity and smaller elastic modulus (The Transtec Group, Inc., 2004). The performance of CRCP is defined in terms of crack width, crack spacing and steel stress for different pavement slab thicknesses and reinforcement design. New design standards assign different percentages of steel for different coarse aggregate types in order to obtain similar crack spacing for different coarse aggregate types (Suh, Hankins, & McCullough, 1992).

In one new CRCP design, 7 in. thick shoulder covered with 1 inch Hot Mix Asphalt (HMA) is connected to the mainline with tie bars. These stronger shoulders cause the CRCP mainline pavement changes this loading condition from an edge loading condition to an internal loading which results in less deterioration in the mainline pavement. The CRCP shoulders significantly improved the pavement life and performance. Figure 2.4 shows the new shoulder design (The Transtec Group, Inc., 2004).

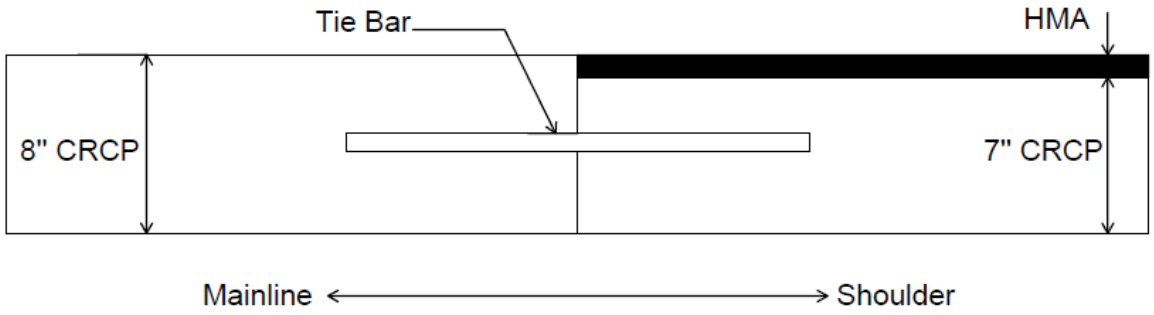

Figure 2.4 New CRCP with shoulder design
After (The Transtec Group, Inc., 2004)

The common deteriorations in CRCPs are punchouts, spallings, and base material pumping. Using tied shoulders to decrease stresses developed by traffic loading; using high quality aggregates to improve cracking pattern; and the use of penetrable and non-erodible base materials decrease punchouts and pumping. CRCP design is associated with computing the width and thickness of the pavement slab and shoulder, longitudinal and transverse steel bars and pavement transitions (ERES Consultants, Inc., 2001).

Potential Causes of Y-Cracking

Y-crack has been considered aprimary cause for punchouts in CRCPs. There are several factors that can contribute to occurrence of Y-cracks.

Crack Spacing

Experiments in 29 states of U.S show that the average spacing between transverse cracks in CRCPs varies from1 to 6 ft. The ideal average crack space is considered to be between 3 to 5 ft. Concrete panels smaller than 0.6-1 m are the most probable panels for punchouts, when load transfer and lower layers support are weakened (Kohler E. E., 2006). CRCP slab panels typically distribute stresses due to external loads (traffic loading) in both longitudinal and transverse

directions. When closely-spaced transverse cracks happen, the CRCP panel will work like a beam with a longer dimension on the transverse direction. As a result, when there is traffic loading, there will be a high amount of transverse flexural stresses which can lead to punchouts. Crack spacing is a sensitive factor which can affect crack width too. Larger spaced cracks can cause larger crack widths, which can lead to more spallings and more intrusion of incompressibles. AASHTO CRCP design guidelines suggests a crack spacing ranges from 1.1 m to 2.4 m (3.5 to 8 ft.) to have the least amount of punchout and spalling distresses (ERES Consultants, Inc., 2001). If stress in concrete slabs reaches the tensile strength, cracks will occur in concrete. TxDOT did some research and found that space between cracks reduces considerably in the first 30 days after placement of concrete due to low strength during the concrete early ages. It was found that crack spacing and concrete strength are related and concrete with lower strength contribute to smaller crack spacing (The Transtec Group, Inc., 2004). Wide cracks reduce aggregate interlock and load transfer. If a wide width transverse crack occurs close to the next transverse crack, the decrease in aggregate interlock will cause increased stresses at the top layer of the concrete when concrete is exposed to the external load. This process can result in punchouts in CRCPs (Kohler & Roesler, 2004). A small amount of steel can cause slightly smaller spaced cracks than plain concrete. To only consider crack spacing in CRCPs, 0.55 to 0.70 percent of steel showed a good performance of the pavement. Results from the experiment done in Vandalia indicated that the higher the percentage of the steel caused shorter crack spacing. The same total amount of strain from thermal and moisture effects needs to be accommodated, regardless of the presence of steel. If steel is present that keeps the individual crack widths small, then there must be a higher amount of cracks to accommodate the

same total strain as in plain concrete. Figure 2.5 shows the results of the experiment done in Vandalia related to the effect of the steel percentage on crack spacing (Kohler & Roesler, 2006).

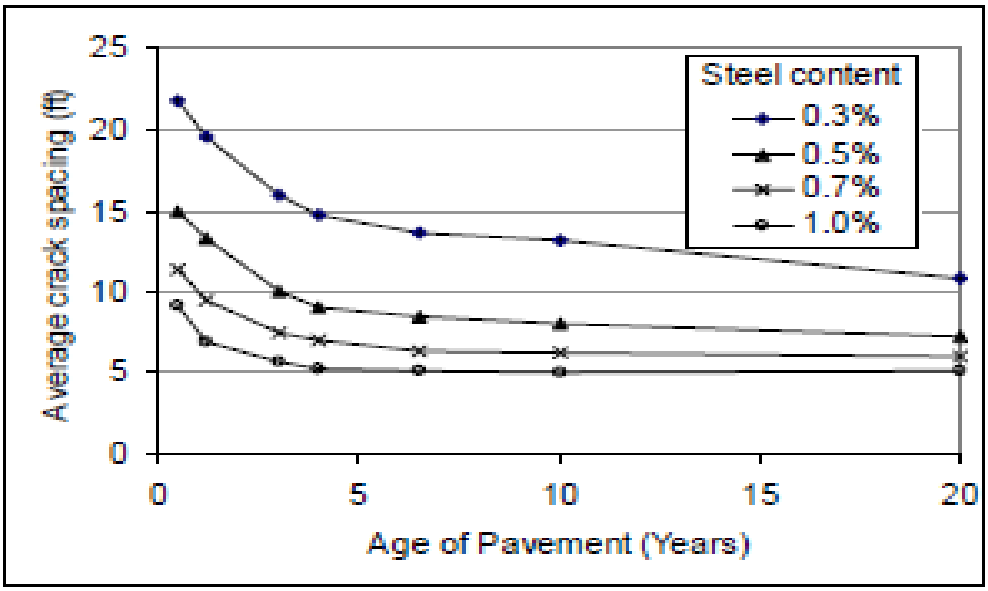

Figure 2.5 Crack spacing over time for various steel percentages for CRCP placed on soil (Kohler & Roesler, 2006)

Also, depth of longitudinal steel in concrete has an effect on crack spacing. The changes in volume of the concrete due to shrinkages are bigger at the concrete surface and reduce with depth. The steel embedded close to the concrete pavement surface resists more the movements induced by shrinkages which lead to higher number of cracks. Also, comparison of data resulted from surveys in South Dakota CRCPs indicated an average crack spacing of 1.7 feet for a pavement with longitudinal steel embedded 2.5 inch below the surface and 2.9 feet for a pavement with steel bars 3.68 inch below the surface (Kohler & Roesler, 2006).

Crack Width

Crack width substantially affects CRCP life and performance. Since crack width is a very effective parameter on pavement performance, it has become a governing element in CRCP

design (Suh, Hankins, & McCullough, 1992). Width of crack has been considered a significant factor because of having effect on load transfer efficiency, water and incompressibles penetration (Kohler & Roesler, 2004). Penetration of water into the pavement through cracks can cause corrosion of the steel bars and weakening of support layers. Entering incompressibles into the wide cracks can result in excessive stresses due to contraction, expansion, and traffic loading, which may cause spalling eventually (ERES Consultants, Inc., 2001). Large crack width causes loss of aggregate interlock which can lead to excessive deflection. Excessive deflection causes distortion in the support layers, which can contribute to base erosion and ultimately punchouts (Kohler E. E., 2006). The AASHTO-86/93 guidelines suggest a maximum crack width of 1 mm (0.04 in) to minimize spalling. However, to avoid water penetration, thus minimizing corrosion of the reinforcement and keeping acceptable load transfer efficiency, AASHTO-86/93 recommends a maximum crack width of 0.6 mm (0.024). Wider cracks may not give problems in freezing temperatures, since frozen surroundings will limit infiltration of water through cracks. Nevertheless, wider cracks may not be acceptable where deicing salts can enter into the crack (ERES Consultants, Inc., 2001). Crack spacing can directly affect crack width due to concrete bends and warps caused by drying and thermal shrinkages. The depth that reinforcements are embedded in the pavement can affect the crack width.

McCullough and Dossey state that early age cracks (primary cracks) are wider cracks. Two factors may be the reasons for larger crack width in early-age cracking:

1. There is no strong bond between concrete and steel at early ages.
2. Because of larger panel dimensions, crack opening movement is larger (Kohler & Roesler, 2004).

In an experiment done by Young-Chan Suh and B. Frank McCullough, the following factors have been considered effective on the crack width. These factors were experimented while other factors kept unchanged.

Concrete Placement Temperature and Season

Concretes with two opposite placement seasons (summer and winter) were compared to see the effect of placement season on crack width. The results indicated that, the crack width in a concrete placed in the summer is much larger than concrete placed in the winter. This could happen due to high curing temperature in summer time (Suh, Factors Affecting Crack Width of Continuously Reinforced Concrete Pavement, 1994). Generally, higher placement temperatures contribute to larger crack widths when the concrete temperature reaches to its normal temperature. Also, Shindler and McCullough in their studies on Texas rigid pavements reflected the effect of air temperature on crack width. Figure 2.6 summarizes their results for effect of air temperature on crack width (Kohler & Roesler, 2006).

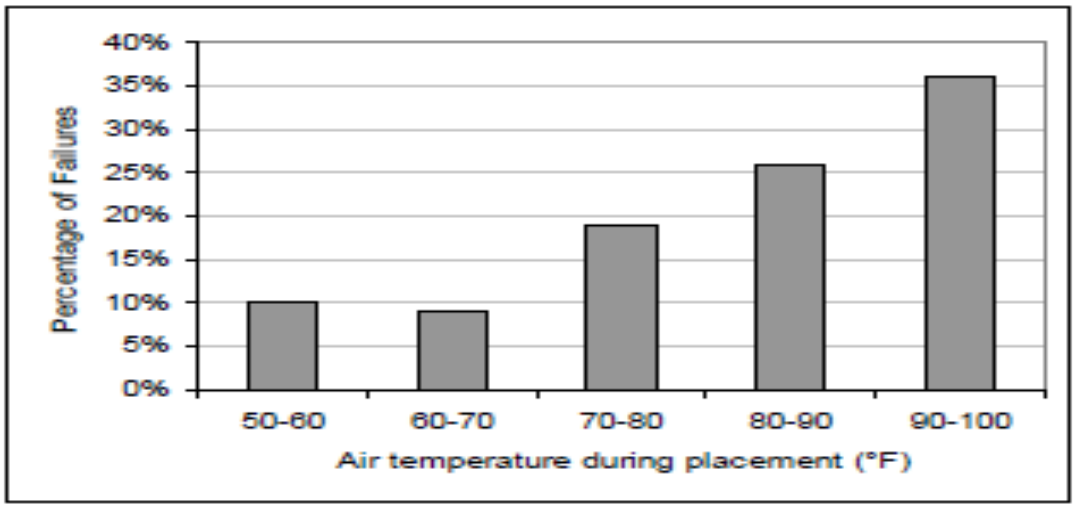

Figure 2.6 Effect of air temperature during placement on long-term CRCP performance in Texas

(Kohler & Roesler, 2006)

Coarse Aggregate Type

Coarse aggregate type affects Coefficient of Thermal Expansion (CTE), shrinkage, modulus of elasticity, and strength of concrete pavement. Experiments done by Young-Chan Suh and B. Frank McCullough showed that use of Siliceous River Gravel (SRG) as coarse aggregates consequences a larger crack width than the use of Lime Stone (LS) and as it can be seen in Figure 2.7 difference was greater at lower temperatures (Suh, Factors Affecting Crack Width of Continuously Reinforced Concrete Pavement, 1994). These results were because of higher Coefficient of Thermal Expansion (CTE) and weaker bond characteristics of SRGs (Kohler & Roesler, 2006).

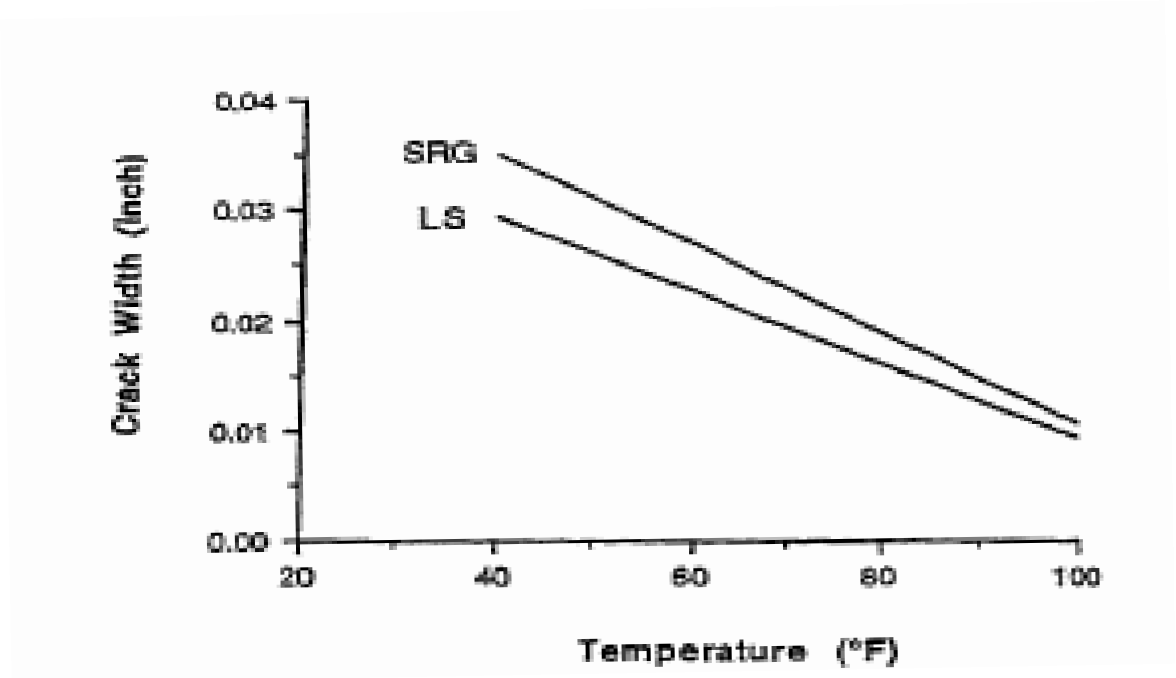

Figure 2.7 Effect of coarse aggregate type and slab temperature on crack width After (Suh, Factors Affecting Crack Width of Continuously Reinforced Concrete Pavement, 1994)

Drying Shrinkage

Drying shrinkage causes cracking in reinforced concrete, especially during the first few days after placement. This cracking continues as long as there is still drying shrinkage. The concretes weak tensile strength and high drying shrinkage of new concrete contribute substantially to cracking. Effective factors on drying shrinkage are water-cement ratio of concrete, rate of hydration, moisture diffusivity, and curing method (Kohler & Roesler, 2006).

Effect of Bond-Slip between Concrete and Steel

Bond stress between concrete and steel is one of the main difficulties in precise modeling of CRCP performance. Bond stress is the interfacial shear stress between the surface of steel bars and concrete which affects crack width. Crack width reduces as the bond between steel and concrete increases (Kohler & Roesler, 2006).

Steel Reinforcement

Several parameters related to steel bars affect crack width in CRCPs. Parameters such as amount of longitudinal steel, number of steel bars, and depth of cover can control crack width (Kohler & Roesler, 2006).

Amount of Steel

Longitudinal steel was really an effective factor in controlling crack width. The higher amount of longitudinal steel resulted in the tighter cracks. This is mainly because of greater bond surface between steel bars and concrete and steel stress (Suh, Factors Affecting Crack Width of Continuously Reinforced Concrete Pavement, 1994). Figure 2.8 compares crack widths for different steel percentage in a 7 in. concrete slab.

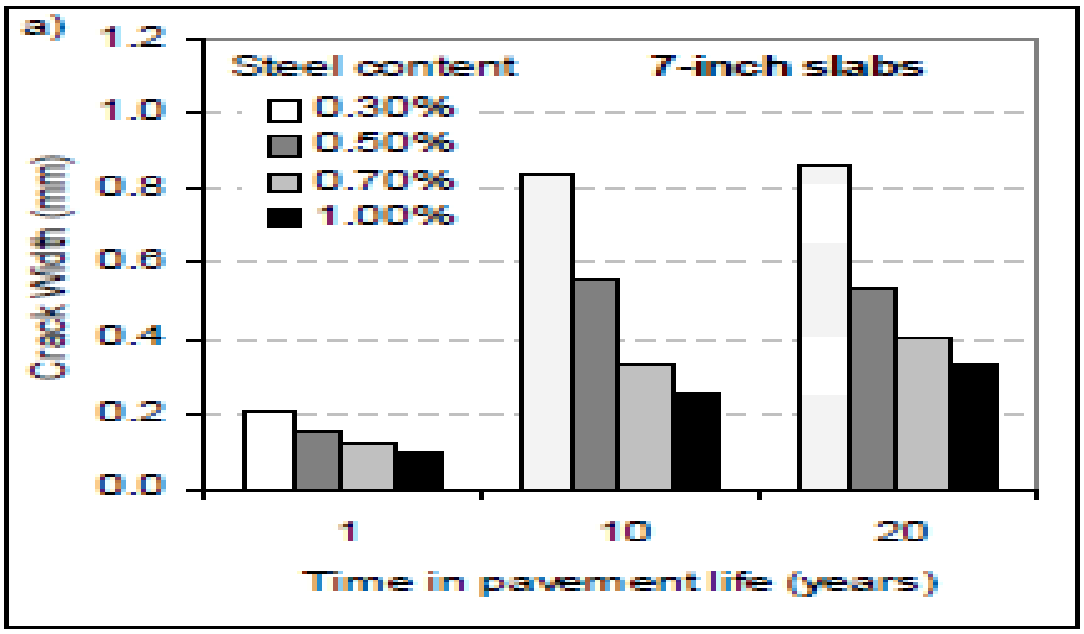

Figure 2.8 Crack width for different steel percentages in a 7 in. concrete slab (Kohler & Roesler, 2006)

Also, crack widths in CRCPs with high, medium, and low amount of steel were compared. From comparisons, it was found that there is no significant difference in crack width between CRCPs with high and moderate percentages of steel. However, the crack width in CRCP with moderate steel percentages was much lower than CRCP with a low percentage of steel (Suh, Factors Affecting Crack Width of Continuously Reinforced Concrete Pavement, 1994).

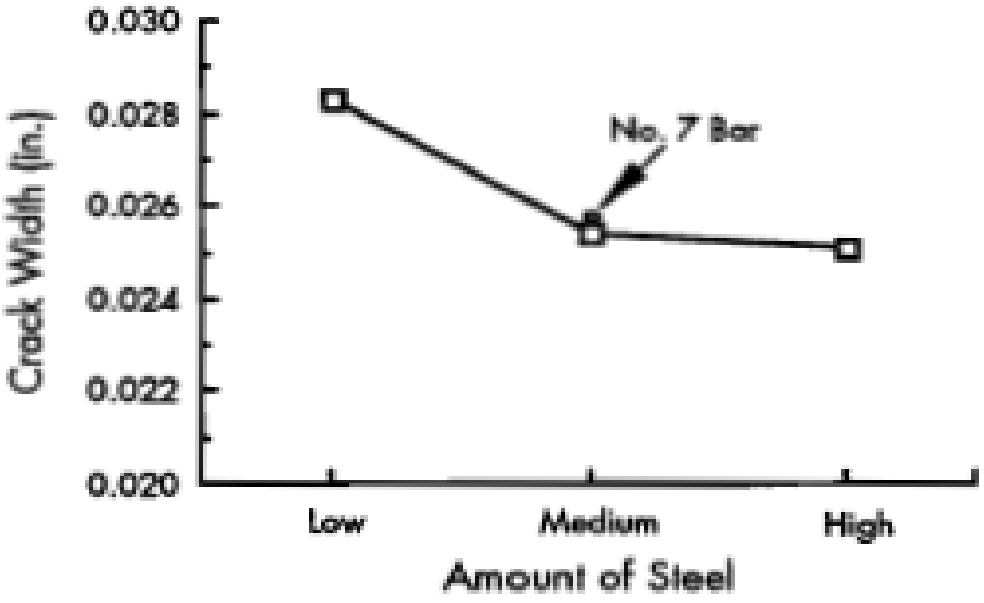

Figure 2.9 Effect of longitudinal steel design on crack width
After (Suh, Factors Affecting Crack Width of Continuously Reinforced Concrete Pavement, 1994)

Steel Bar Size

Also, steel bar size had a large effect on crack width. Larger bar sizes resulted in wider cracks when the total amount of steel was fixed. The reason for this can be the lower surface for bonding between concrete and steel with the larger bar size (Kohler & Roesler, 2006).

Time of Crack Occurrence

Results from experiments showed that cracks that happened in the first three days after building the pavement were considerably wider than those cracks that happened at later ages. Drying shrinkage is thought to be the main reason for larger width of cracks that form at early ages. The crack width grows with as the concrete dries after the occurrence of crack, which means early age crack is wider due to having a higher remaining drying shrinkage than a later

age crack (Suh, Factors Affecting Crack Width of Continuously Reinforced Concrete Pavement, 1994)

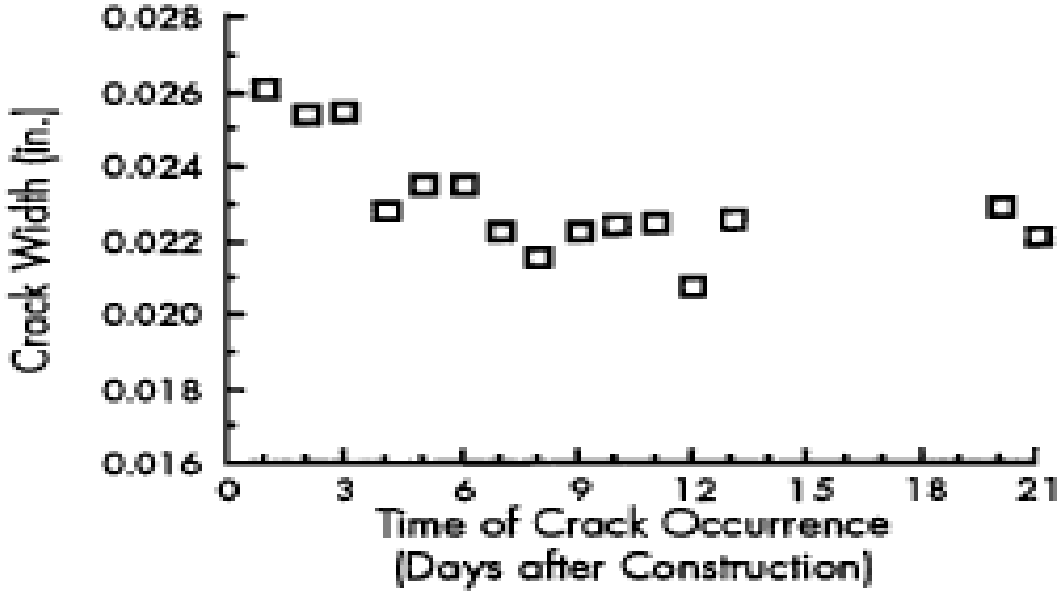

Figure 2.10 Effect of time of crack occurrence on crack width
After (Suh, Factors Affecting Crack Width of Continuously Reinforced Concrete Pavement, 1994)

Pavement Support

A common mechanism that leads to a weak base support is the pumping of base materials through cracks and joints. The pumping can cause a weak base support and as result punchouts and spalling in pavement. In order to prevent from pumping, it is specified to build base layers with non-erosion materials for CRCPs exposed to heavy traffic loads. Common base types for CRCPs performed very well under heavy traffic were open-graded drainable bases, asphalt treated bases, and cement treated bases. Another characteristic that a good base material may have is to have a high permeability. A permeable base material allows water to be drained quickly; that reduces the time of saturation which is the time of weak base support. Some of the

problems seen about these drainable bases were pumping of lime-stabilized subgrades into the drainable base, early age cracking and weak performance of CRCP on cement-treated drainable bases (ERES Consultants, Inc., 2001).

Chapter 3 Methodology

Pavement Stress Modeling

Finite element methods (FEMs) were used to model the change in principal stress direction based on design and construction conditions. The modeling was undertaken to determine any changes in stress direction or concentrations that occur from changes in design and construction. It is expected that any changes in the stress magnitude will influence spacing of cracks and time corresponding to crack initiation. Changes in the maximum principal stress direction will cause a change in the crack direction, potentially causing y-cracking. A change in the distribution of the maximum principal stress across the pavement width will also cause cracks to meander and contribute to y-cracking.

The computational model of a pavement was assembled including concrete, subbase, and subgrade. Models were also assembled with patches of differing subbase friction, shoulders, and different amounts of reinforcing steel. The finite element software package used consists of several modules, which enable the complete formulation of the computational model including pavement geometry and mechanical properties. The analysis module performs the finite element calculations and creates an output data base (odb) file. The output data base file is then used to access the results and determine changes in the stress distribution and principal stress directions.

3.1 Pavement Structure Finite Element Model

A FEM was built for CRCP pavement structures in Oklahoma. The pavement geometry and layer properties were based on typical values of Oklahoma CRCP. Pavement layers were 3-Dimensional, linear elastic layers. The pavement consisted of three layers: 144 in. wide, 10 in. thick concrete pavement (surface layer); a 216 in. wide, 4 in thick asphalt concrete (AC) subbase

layer; and a 288 in. wide, 36 in thick soil subgrade layer. There was no shoulder for the basic finite element model. Figure 3.1 shows the computational model used in the analysis.

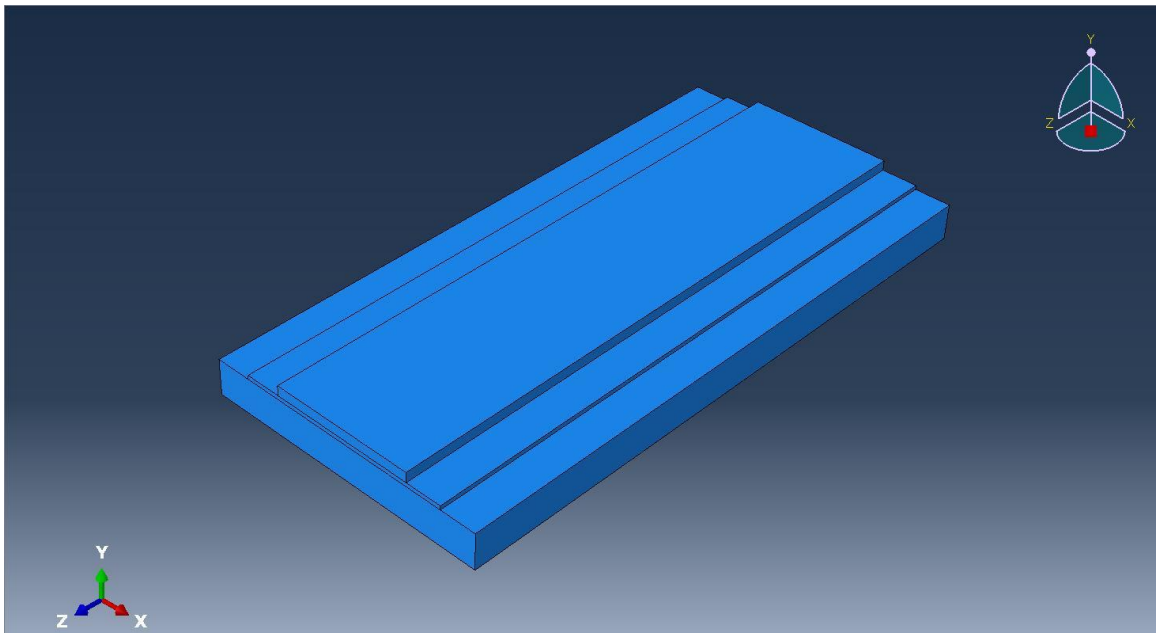

Figure 3.1 Pavement model created by Abaqus/CAE software package

Mechanical and thermal parameters defined for each material were: young's modulus (E), Poisson's Ratio (ν), coefficient of thermal expansion (CTE), mass, density and thermal conductivity. Table 1 summarizes the layer geometry, mechanical and thermal parameters for each material used in the finite element model.

Table 1 Pavement layer geometry, mechanical, and thermal properties

Inputs	Pavement(Concrete)	Subbase(AC)	Subgrade(Soil)
Young's Modulus E(psi)	3122019	435000	4000
Poisson's Ratio ν	0.17	0.4	0.3
Coefficient of Expansion CTE(1/F°)	6.00E-06	1.38E-05	5.00E-06
Mass Density(Ib/ft^3)	4.4928	4.6656	3.2832
Thermal Conductivity(Btu/in.hr.F°)	0.0616	0.0361	0.0385
Length(inch)	600	600	600
Width(inch)	144	216	288
Thickness(inch)	10	4	36

Two interactions were created for these three layers in the model. A surface to surface contact with friction coefficient of 20 was defined for the interaction between pavement layer and subbase layer. Another interaction was defined using the same procedure with a friction coefficient of 20 for the interaction between the subbase and subgrade layers. Figure 3.2 shows the location of the interactions between the pavement and subbase. Figure 3.3 shows the location of the friction interactions between the subbase and subgrade. Since materials and interactions were similar to those used by (Timm, Guzina, & Voller, January 2003), friction coefficient values were obtained from models in that paper.

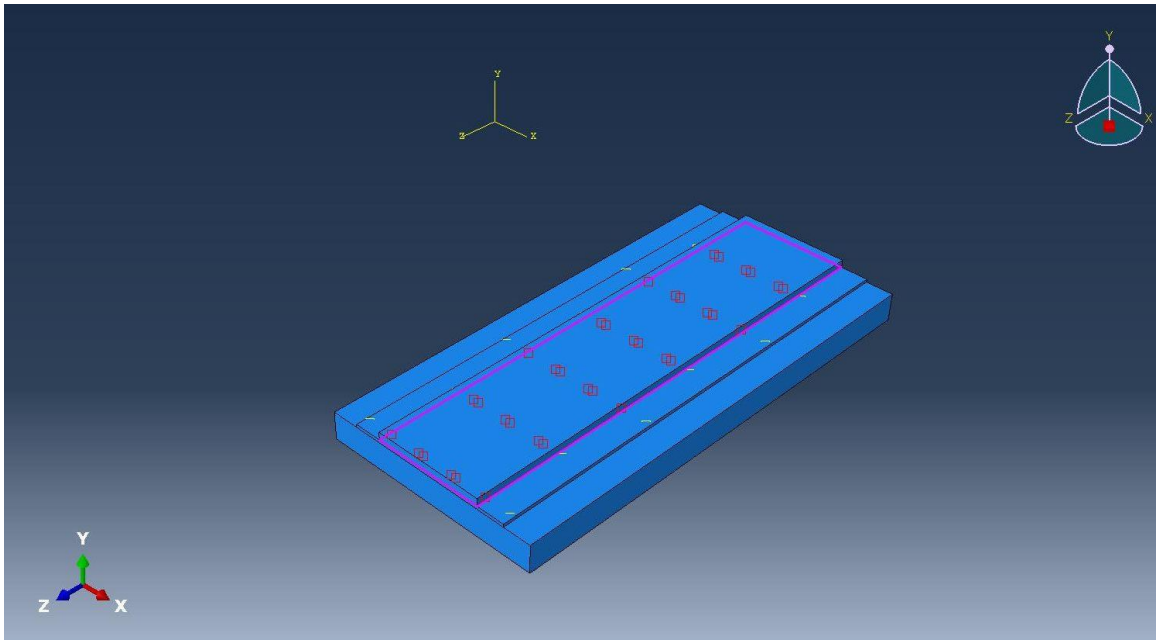

Figure 3.2 Friction interaction location between pavement and subbase

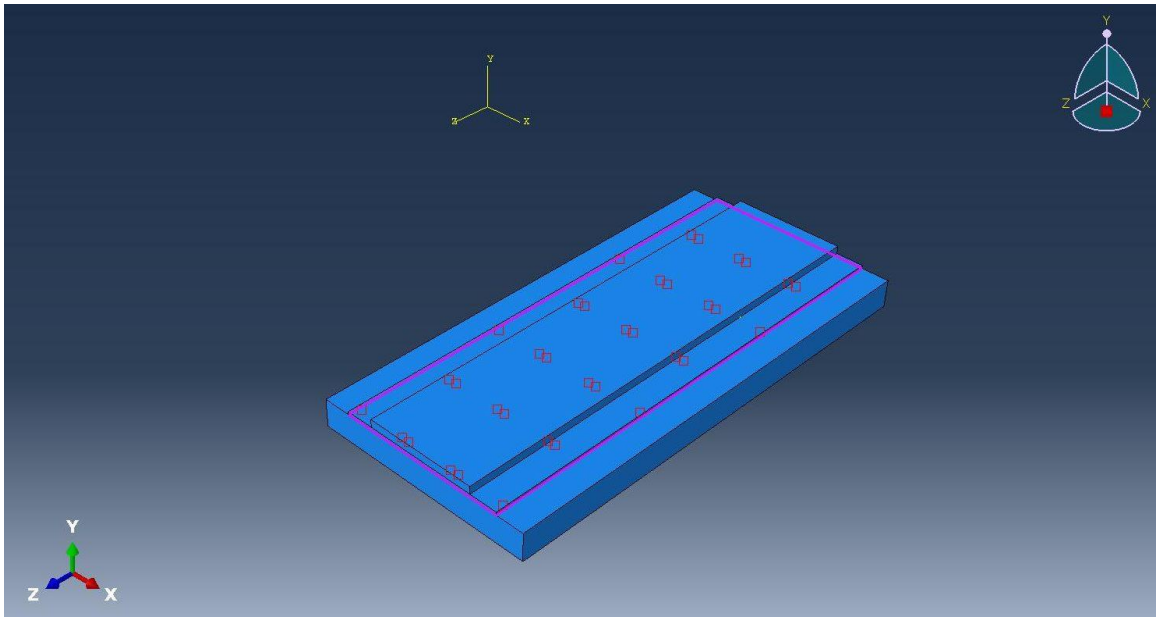

Figure 3.3 Friction interaction location between subbase and subgrade

The bottom of the subgrade was fixed against displacement in all directions and rotation as shown in Figure 3.4. Subgrade sides were restrained against displacement in the transverse and longitudinal directions as shown in Figures 3.5 and 3.6.

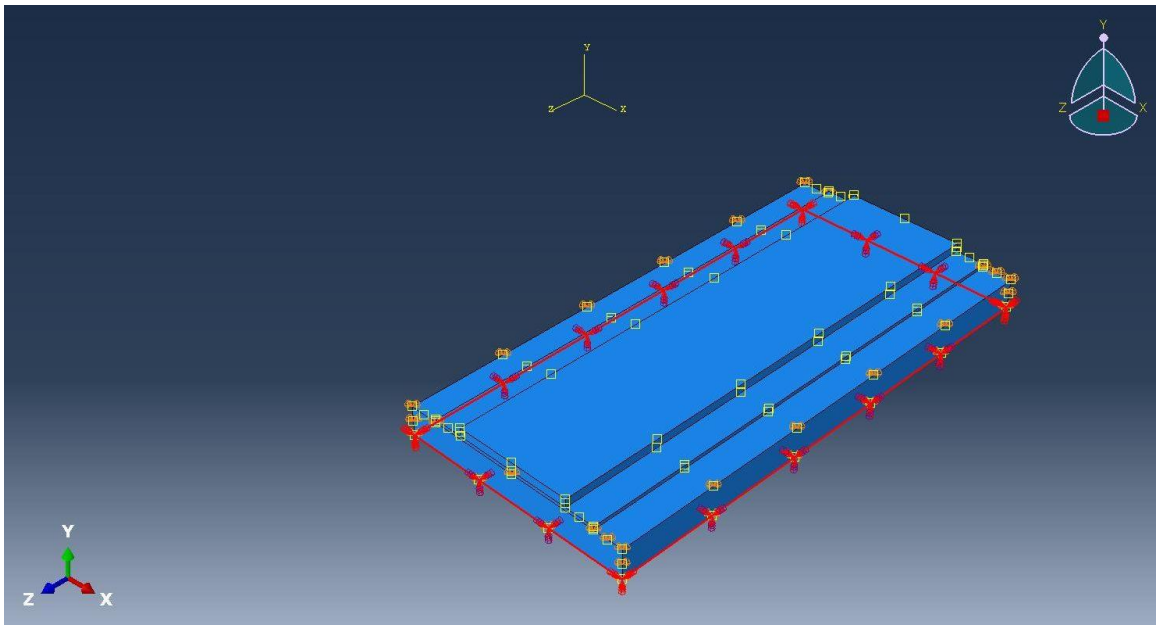

Figure 3.4 Boundary conditions at the bottom of the subgrade

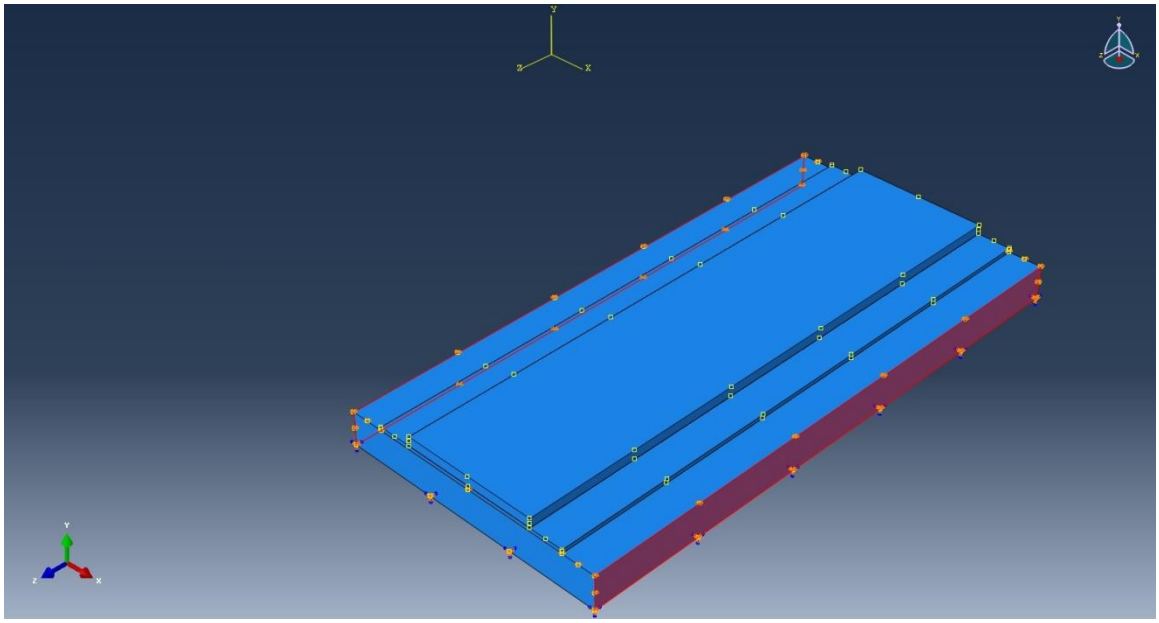

Figure 3.5 Boundary conditions on the subgrade longitudinal direction sides

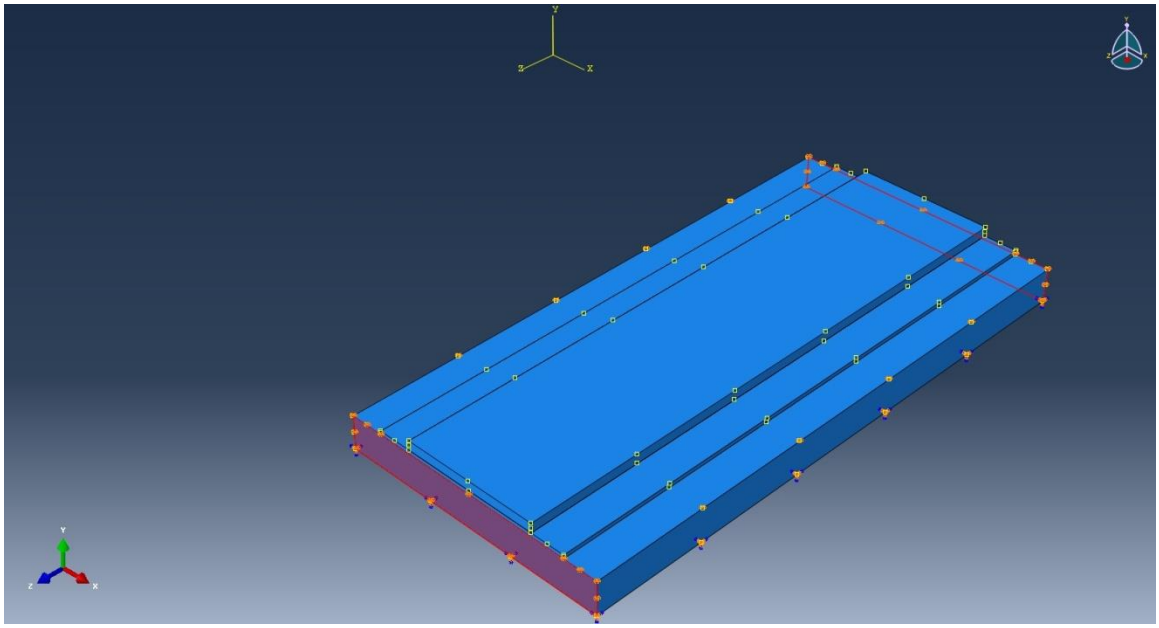

Figure 3.6 Boundary conditions on the subgrade transverse direction sides

The gravity load was applied uniformly to the whole model. The gravity load with a vertical acceleration component of 386 in/s2 was applied downward to the whole model as shown in Figure 3.7. It is essential to apply the gravity load to ensure that the friction between layers is engaged. A temperature decrease of 50° F was applied to concrete pavement while the temperature underneath the pavement was kept constant. This temperature loading was used to simulate the effects of drying shrinkage and temperature change seen by the pavement and not by the subbase and subgrade. The primary purpose of this modeling is to determine the stress distribution patterns. This will show if there are locations that are prone to higher densities of cracks or cracks with a tendency to change direction for crack branching.

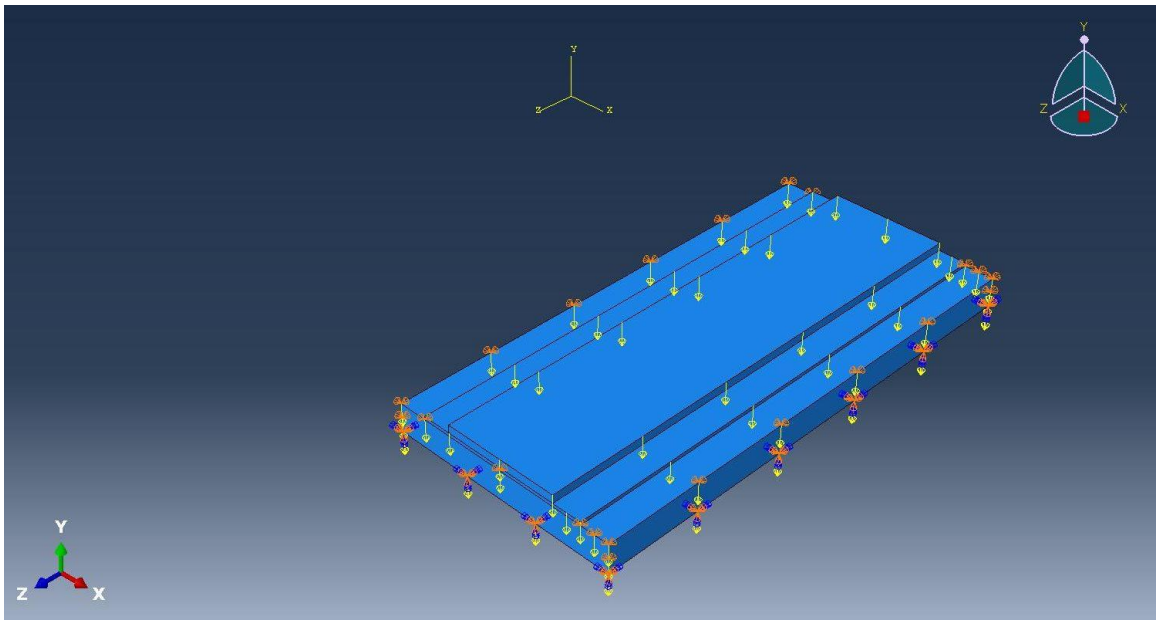

Figure 3.7 Gravity load applied uniformly to the pavement and substructure

Coupled Temperature-Displacement elements were used in this finite element model. A 6 in. seed size was used for the automatic meshing using 8 node cubic elements. Figure 3.8 shows the finite element mesh used for the mainline pavement section. This mesh was used for all three layers in model. The number of elements used for the pavement (surface layer), subbase, and subgrade were 4,800, 3,600 and 28,800 respectively.

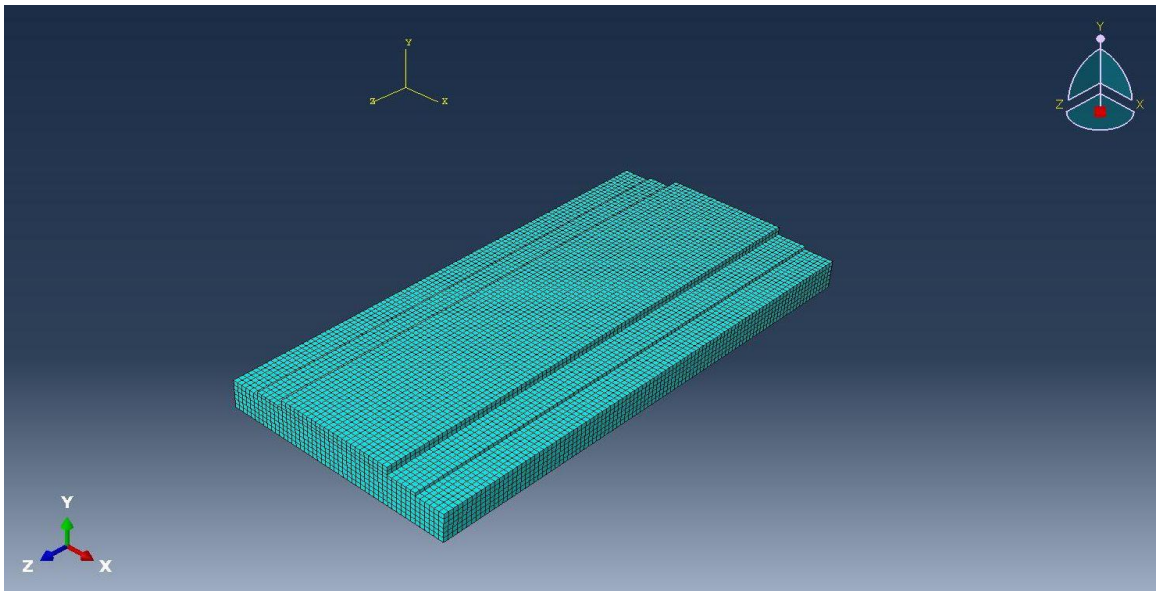

Figure 3.8 Mainline pavement lane model mesh

Load was applied in two steps: 1) gravity load, 2) thermal load in the presence of gravity.

At this stage, model was ready and it was submitted for running. The results of models are in result chapter.

3.2 Effect of Localized Changes in the Layer Interfaces

A localized change in friction between the concrete and supporting layers was modeled to determine how subbase construction uniformity could affect y-cracking. The impact of these patch properties on the maximum principal stress direction was studied by varying the location of patch in the pavement, patch size, and friction coefficient (FC) of interaction between patch and the underlying layer.

3.2.1 Patch Location

Patches or locations of different interface frictions were placed at two different locations in the pavement: a patch at the corner of the pavement and a patch at the longitudinal edge in the

middle of pavement. Figure 3.9 shows the location of changed friction areas at the corner and middle of the pavements, respectively.

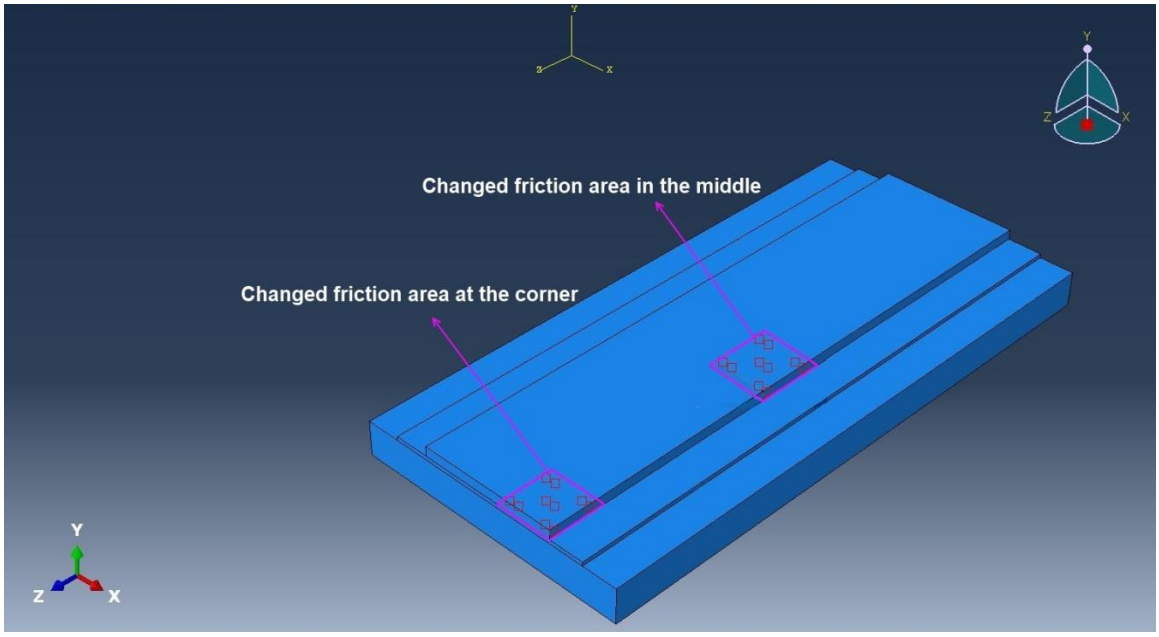

Figure 3.9 Location of changed friction areas at the pavement corner and at the longitudinal edge in the pavement middle

Patch sizes used were 3’ x 3’, 5’ x 5’ and 7’ x 7’. Friction coefficient (FC) of interaction between patch and subbase for all patches was 1, while FC was 20 for the interaction between the rest of the pavement and subbase. Normal stresses in the transverse direction (S11) were sampled across the width of the pavement

3.2.2 Effect of Patch Size and Its Friction Coefficient

Four models were run to understand the effect of patch size and friction coefficient (FC) on how the direction of maximum principal stresses varies across the width of the pavement. To determine the effects of patch size on stress magnitude and direction, the patch size was changed for the patch at the corner. The patch friction coefficient was then changed for both the 5’ x 5’ and 7’x 7’ patches as follows:

1- Model with a 5’x 5’ patch, patch FC=1, FC=20 for the rest of the pavement.

2- Model with a 5’x 5’ patch, patch FC=20, FC=1 for the rest of the pavement.

3- Model with a 7’x 7’ patch, patch FC=1, FC=20 for the rest of the pavement.

4- Model with a 7’x 7’ patch, patch FC=20, FC=1 for the rest of the pavement.

The principal stress directions across the width of the pavement at the transverse edge were calculated from the finite element output data. After extracting all six components of stress state from the finite element output data, a stress tensor was assembled for calculation of principal stress directions. Angles between maximum principal stress direction and the transverse, vertical and longitudinal axis are referred to as α, β, and γ angles, respectively.

3.3 Pavement with Shoulder

3.3.1 Shoulder without Joints

A 10 in. thick shoulder with 78 in. width was added to the side of the pavement to investigate the effects of shoulders cast after the mainline pavement on y-cracking. The materials used on the mainline pavement were also used on the shoulder pavement. Figure 3.10 shows the model generated for this case.

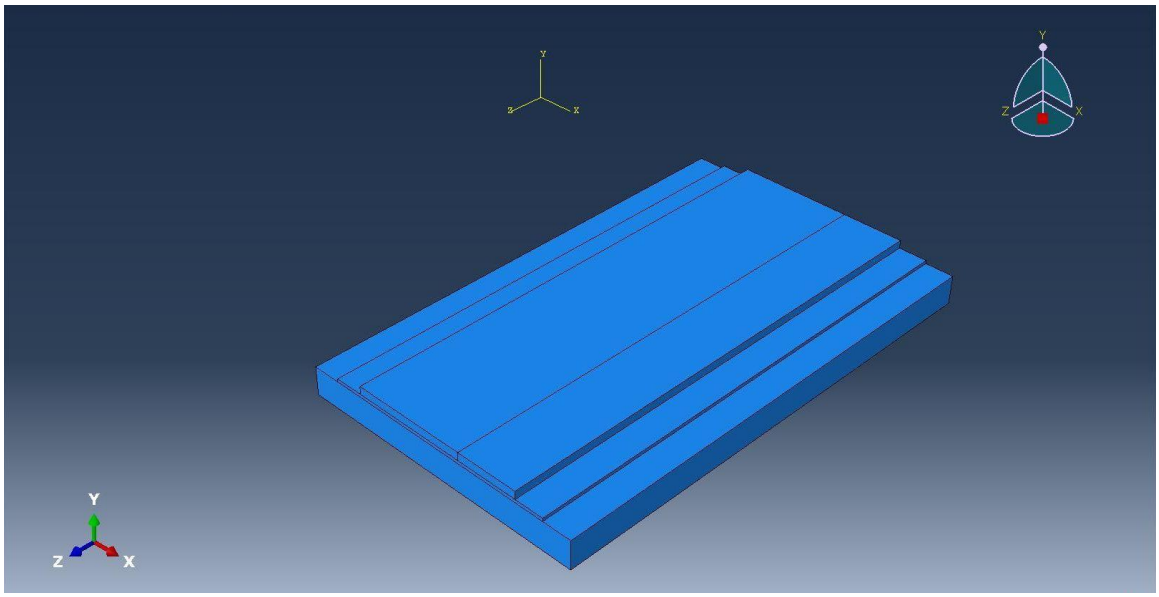

Figure 3.10 Concrete pavement model with CRCP shoulder

Two interactions were created for these three layers. A surface to surface contact with friction coefficient of 20 was defined for interaction between the pavement layer and subbase layer. Another interaction was defined with a friction coefficient of 20 between the subbase layer and the subgrade layer.

The bottom of the pavement structure was completely fixed, thus disabling all displacement and rotation components at this location. Also, the vertical sides of the subgrade were prevented from translating in both transverse and longitudinal directions.

As in the mainline pavement model, the gravity load was applied uniformly to the pavement layers. This gravity acceleration of 386 (in/s2) was applied in the downward vertical direction. It is essential to apply the gravity load to ensure that the friction between layers is engaged.

Coupled Temperature-Displacement elements were used. All elements used were 8 node cubic elements A 6 in. seed size was used during the auto meshing procedure.

A temperature decrease of 50° F was applied to the entire concrete pavement including mainline and shoulder while the temperature for underneath of the pavement was kept constant.

3.3.2 Shoulder with Joints

Another model was assembled for the pavement with jointed shoulders. All parameters were equal to those used in the previous models except for three transverse joints created in the shoulder as shown in Figure 3.11.

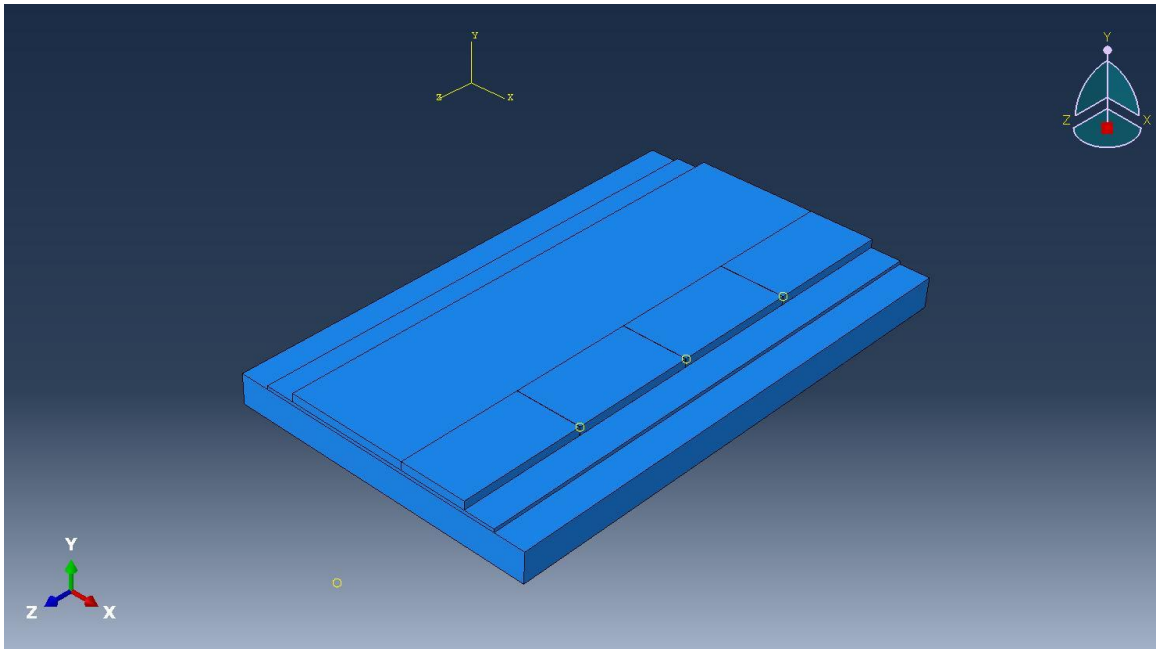

Figure 3.11 Computational model that includes a jointed pavement shoulder

Coupled Temperature-Displacement elements were used in this finite element model, with a 6 in. seed size applied to the automesh function. Elements used in the subbase and subgrade were 8 node cubic elements. Elements in the pavement portion of the model however were triangular because of the geometry imposed by the joint – mainline pavement intersection Figure 3.12 shows the mesh for this model.

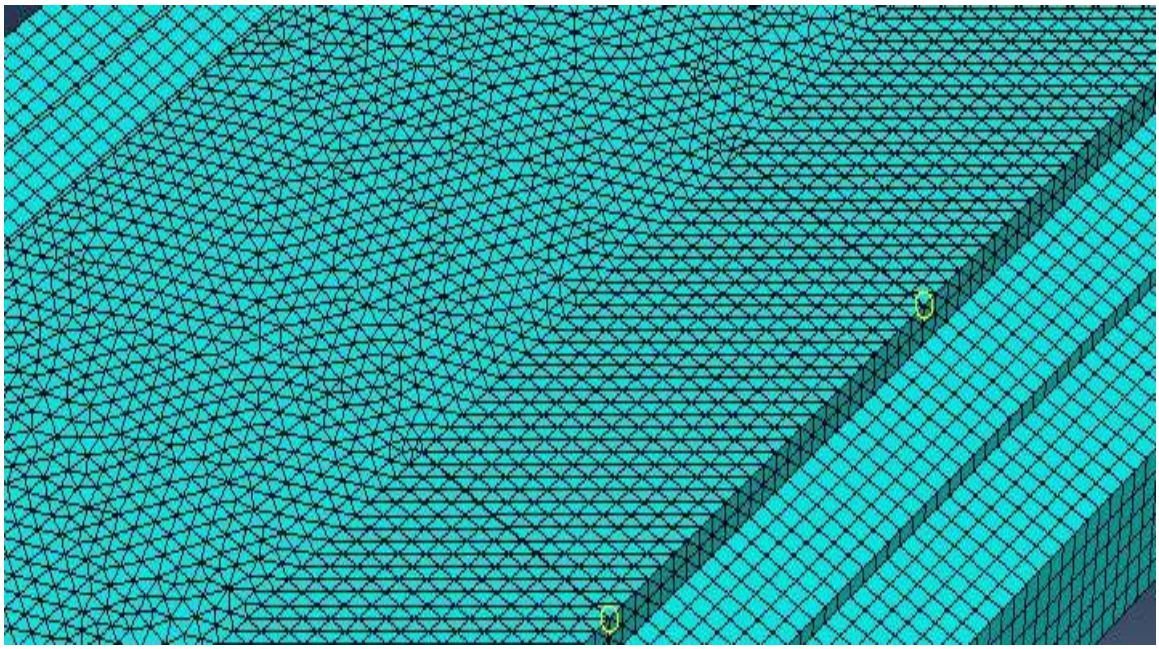

Figure 3.12 Close-up model of jointed shoulder after meshing

A temperature decrease of 50° F was applied to whole concrete pavement including mainline and shoulder while the temperature for underneath of the pavement was constant. The temperature for the pavement layer decreased from 100° F to 50° F, whereas the temperature for subbase and subgrade was constant and equal to 50° F.

3.3.3 Different Shrinkage between Mainline and Shoulder Pavements

Different temperature changes were imposed on the mainline and shoulder pavements in order to simulate the effects of the differential drying shrinkage between the hardened mainline concrete and the newly cast shoulder. A temperature reduction of 50°F was imposed on the shoulder in all models while the temperature reduction for the mainline was varied between 5, 10 and 40° F in all models with continuous shoulder. The subgrade and subbase temperatures were kept constant.

For three models with CRCP shoulders, principal stress directions were calculated at the transverse edge and in the middle transverse cross section. Figure 4.3 shows paths along which that principal stress directions were calculated.

3.4 Model with reinforcement

Two finite element models with two different percentages of longitudinal steel reinforcement were investigated. All other parameters were equal to those in the previous model with continuously reinforced concrete shoulders. 30 longitudinal bars of 0.75 in. diameter were embedded in the pavement for the model with 0.6 % longitudinal steel. Thirty five #6 bars (0.75 in. diameter) were used for the model. This provided 0.7 % longitudinal steel. The transverse steel was #5 bars (0.625 in diameter) with 44 in. spacing. Tie bars that were 30” in length with 30” spacing were used to tie the mainline to the shoulder. Figure 3.13 shows the arrangement of steel bars inside the pavement.

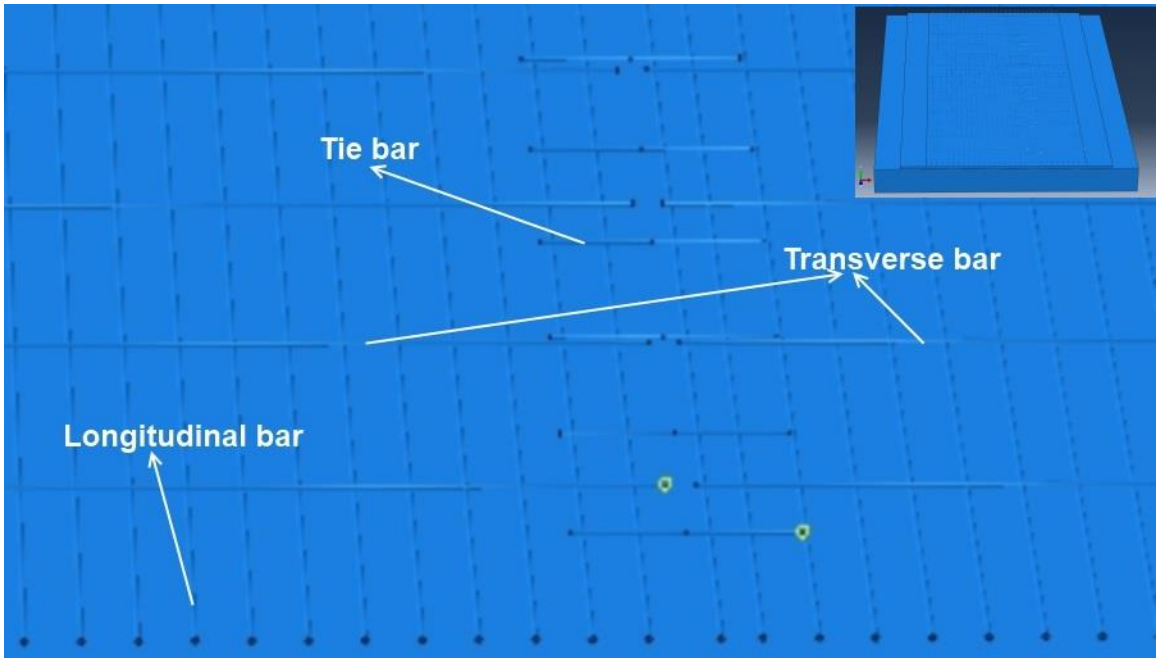

Figure 3.13 Arrangement of steels in the pavement with 0.6 % longitudinal steel

Friction coefficients between all pavement layers were 20 and a gravity load acting downward was applied the entire model to engage the layer interactions. A temperature reduction of 50°F was imposed on the shoulder while the temperature reduction for the mainline was 10°F. The subgrade and subbase temperatures were kept constant.

Chapter 4 Results

Results of Pavement Stress Modeling

4.1 Pavement Structure Finite Element Model

A graphical display of normal stresses in longitudinal direction (S33) is shown in Figure 4.1 and 4.2. The S11, S22, and S33 stresses are the normal stresses in the x, y, and z directions. The reason that stress in the longitudinal direction (S33) is very important to discuss is that S33 is the main component of maximum principal stress in contributing to transverse cracking. Figure 4.1 and 4.2 shows that tensile stresses developed approximately in the central areas (green areas) whereas compression stresses developed approximately at the top transverse edges (blue areas) where the pavement curled upwards. Also, the stress magnitude in the middle of the pavement between two ends was the largest and it started to decrease towards the ends (in the longitudinal direction). Since there was a high tensile stress in the middle of the pavement between two ends, the probability of cracking in the central areas was higher than transverse edges of the pavement. This corresponds to what one would intuitively predict, because of the high restraint experienced by the middle of the pavement from long sections of pavement with subbase friction in the longitudinal direction.

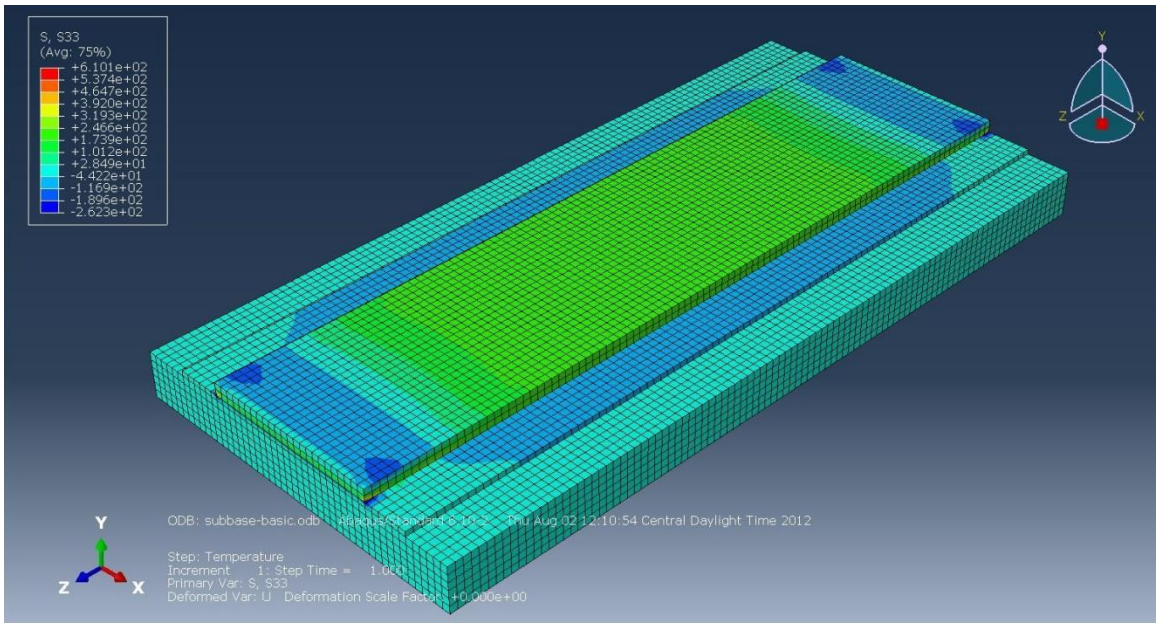

Figure 4.1 Distribution of normal stress in the longitudinal direction (S33)

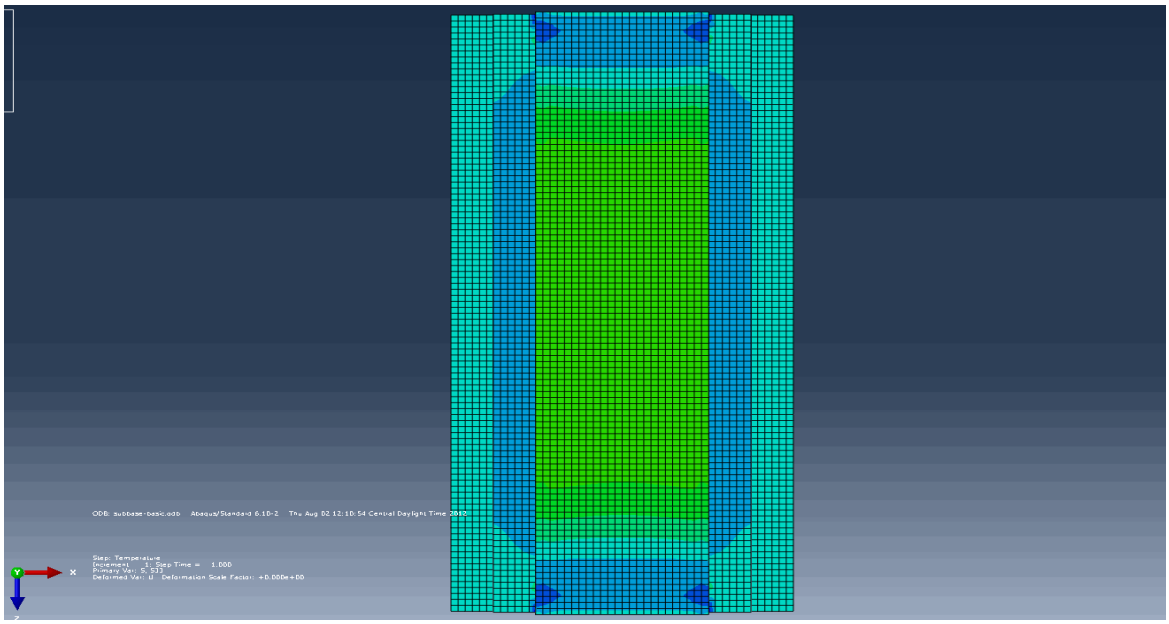

Figure 4.2 2-D plot for distribution of normal stress in the longitudinal direction (S33)

Distributions of stresses and displacements induced by the temperature reduction in the pavement were obtained by sampling the stresses along the transverse directions in the middle and at the edge, paths are shown in Figure 4.3.

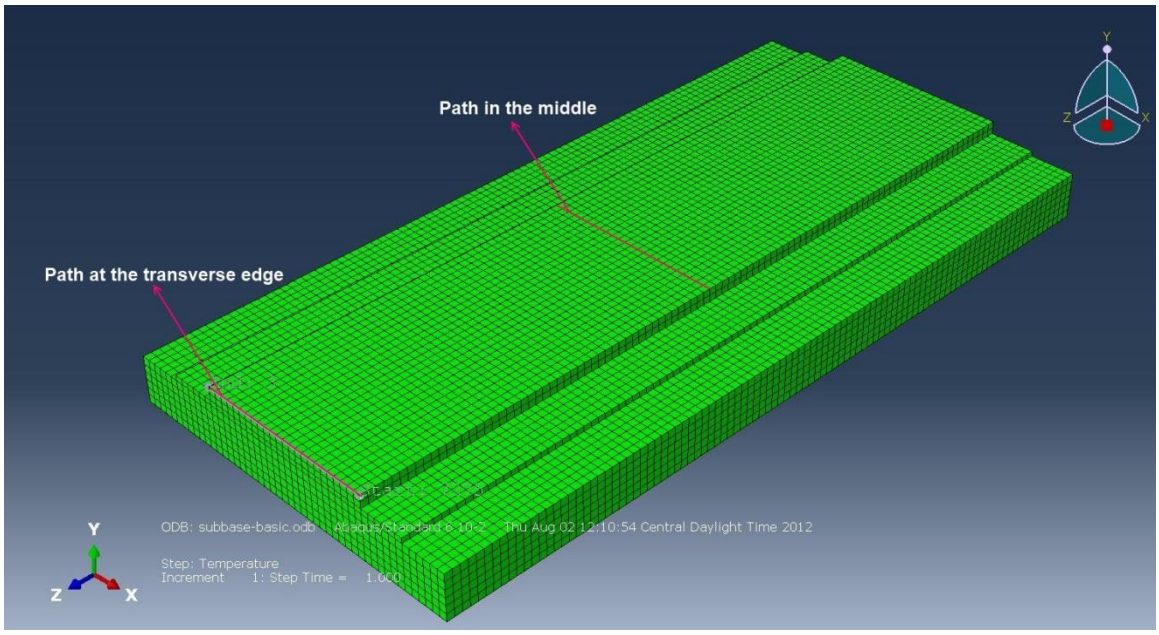

Figure 4.3 Path examined for stress at the pavement transverse edge

Figure 4.4 shows distribution of normal stresses in the transverse (S11) and longitudinal (S33) direction along the width of the pavement in the middle of the pavement section. As seen, the stress in the transverse direction (S11) was symmetric along the width of the pavement and it varies from approximately 16 to 70 psi along the width. Since the quantity of stress is proportional to the length, stresses in the transverse direction were lower than stresses in the longitudinal direction because of the lower restraint created by the shorter length in the transverse direction. Stresses were tensile stress along the width of the pavement.

There is much less of a difference in stress along the pavement width in the longitudinal direction than in the transverse direction. The stresses in the longitudinal direction are also higher, notably because of the higher amount of restraint provided by the pavement length in contact with the subbase in the longitudinal direction.

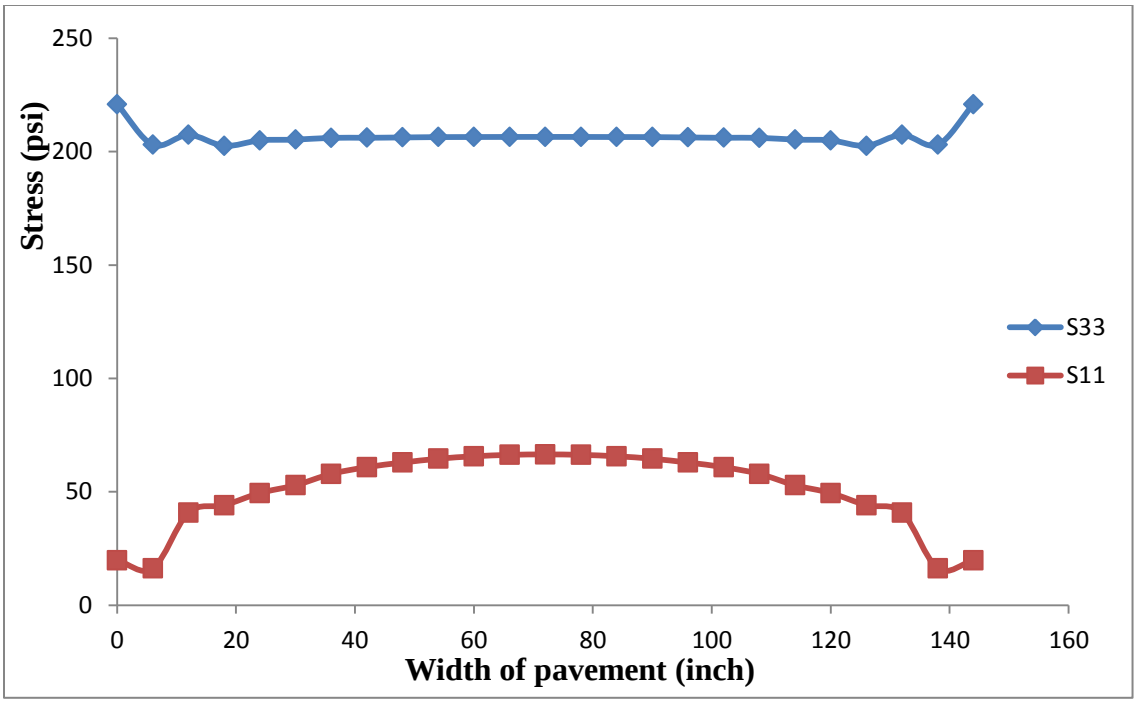

Figure 4.4 Distribution of the longitudinal and transverse normal stress along the width of the middle of the pavement between two ends

Figure 4.5 shows the distribution of longitudinal normal stress (S33) along the width of the pavement at the transverse edge. The S33 stresses are symmetric along the width of the pavement, as expected because of the symmetric pavement modeled. This also shows that the concrete pavement under ideal construction conditions will most likely crack transverse to the pavement and not y-crack.

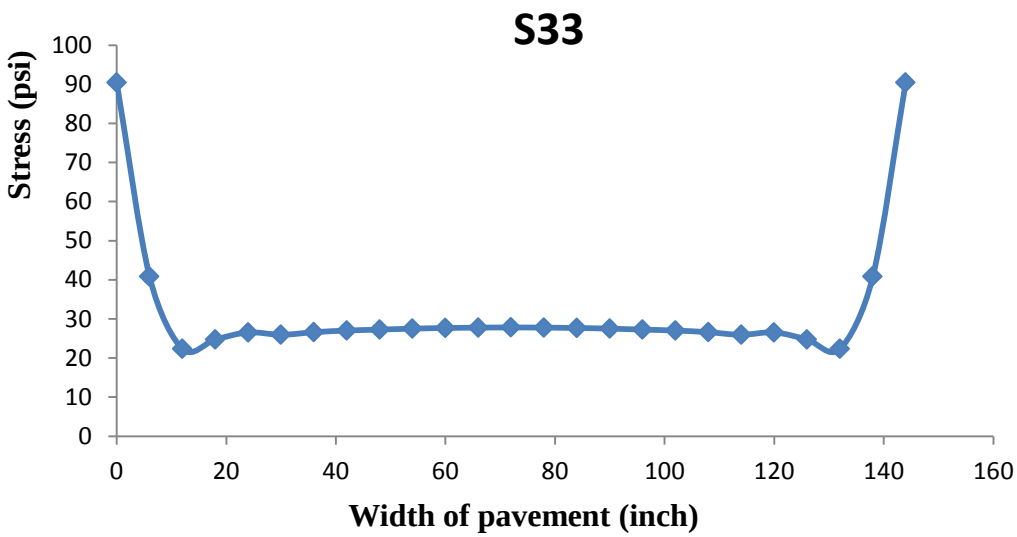

Figure 4.5 Variation of S33 along the width of the transverse edge of the pavement

Figure 4.6 shows that pavement displacement in the transverse direction (U1) is constant along the length of the pavement.

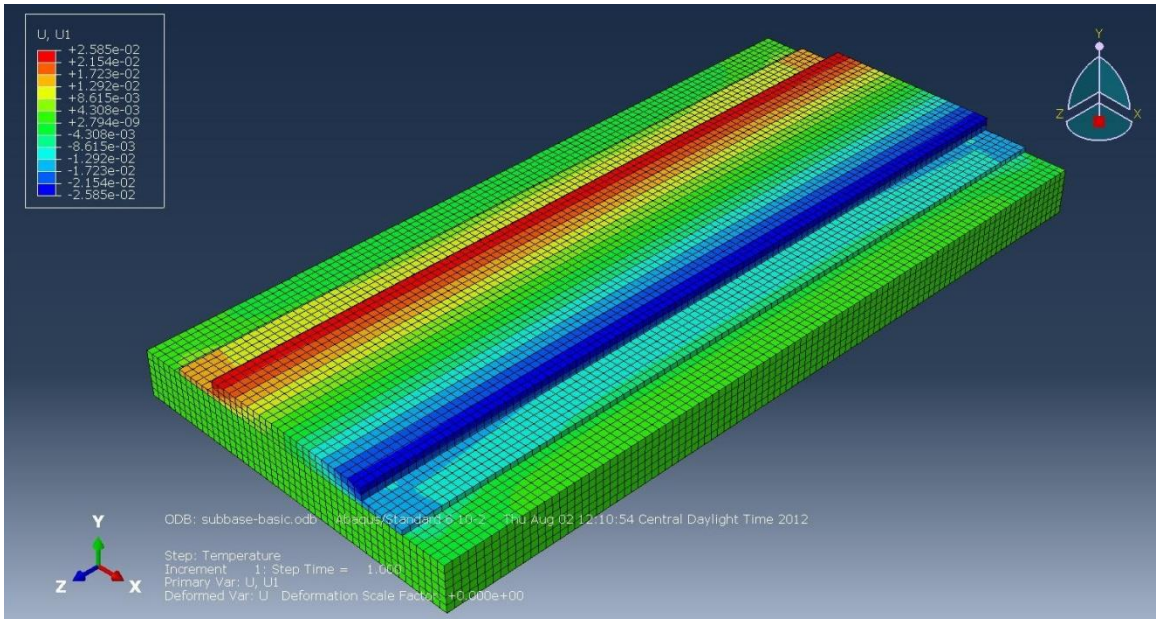

Figure 4.6 Color map of U1 in the whole pavement model.

4.2 Effect of Localized Changes in the Layer Interfaces

4.2.1 Patch Location

Figure 4.7 shows the distribution of the transverse (S11) stress at the edge of patch for patches at the corner and Figure 4.8 shows the change in S11 at the halfway point between the two ends for patches at the longitudinal edge in the middle of the pavement section.

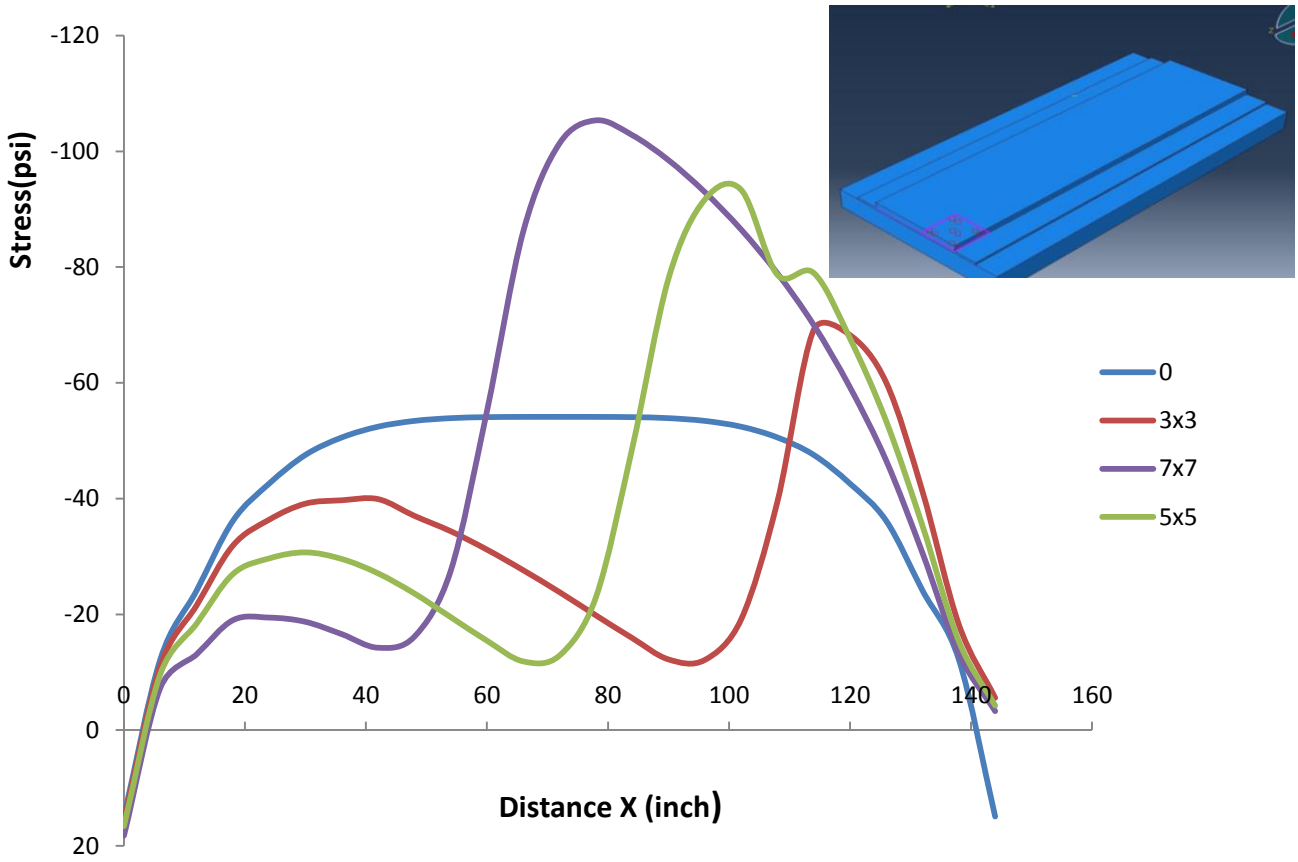

Figure 4.7 Distribution of S11 for patch at the corner (FC-Patch=1 and FC-Rest of the Pavement=20).

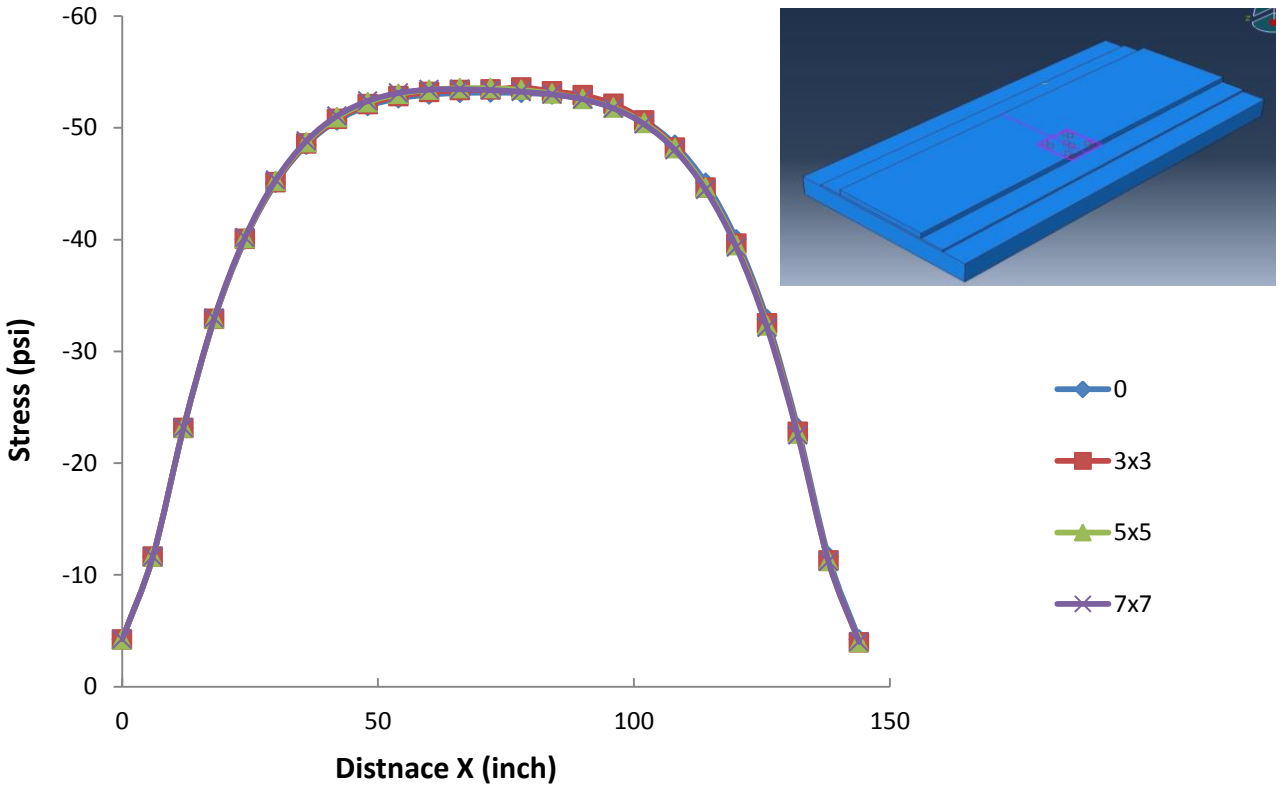

Figure 4.8 Distribution of S11 for patch placed halfway between two ends (FC-Patch=1 and FC-Rest of the Pavement=20)

A change in the friction at the corner had a large effect on the stress magnitude and direction at the edge of the patch. A patch placed halfway between the pavement ends did not significantly change the pavement stress state. As seen in Figure 4.7, the patch size has a large effect on the stress magnitude when the patch is near the transverse edge of the pavement. When the patch location is near the middle of the section between cracks in the longitudinal direction however, the transverse stresses did not change significantly.

4.2.2 Effect of Patch Size and Its Friction Coefficient

Figure 4.9 shows the angle between the maximum principal stress and longitudinal axis (γ angle) across the width of the pavement at the transverse edge for the two models with two different patch sizes.

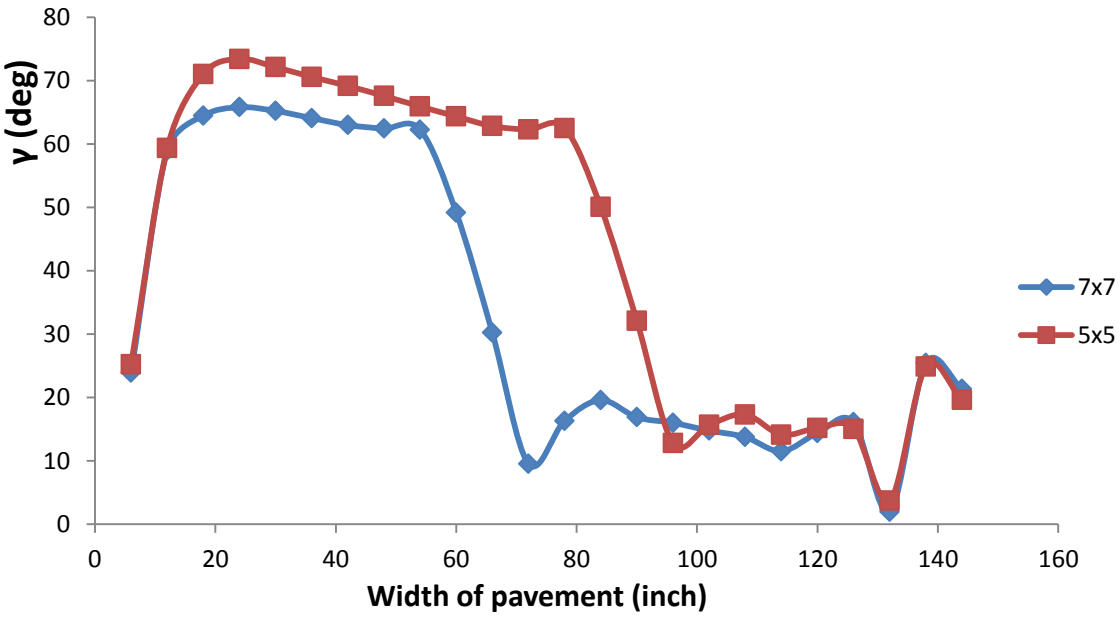

Figure 4.9 Distribution of γ along transverse edge (FC-Patch=20 and FC-Rest of the Pavement=1)

The patches showed an abrupt change in the principal stress direction at 60 in. for the 7'x7' and at 84 in. for the 5' x 5' patch, corresponding to the edge of each patch. Both sections showed principal stress directions at least 25° from the transverse direction, indicating a high potential for branching cracks and Y-cracking.

Figure 4.10 and 4.11 compare two different models with different friction coefficients (FC) for the 7' x 7' patch and 5' x 5' patch, respectively. For these models, FC was changed from 1 to 20, with the FC for the remaining pavement changed from 20 to 1. This data shows

that a change in friction over a section of the pavement, whether an increase or decrease, will give non-uniform restraint and cause the principal stress direction to meander. A decrease or increase in the pavement friction will cause the meandering to go in opposite directions. It appears that a key to preventing y-cracking is subbase surface characteristic uniformity.

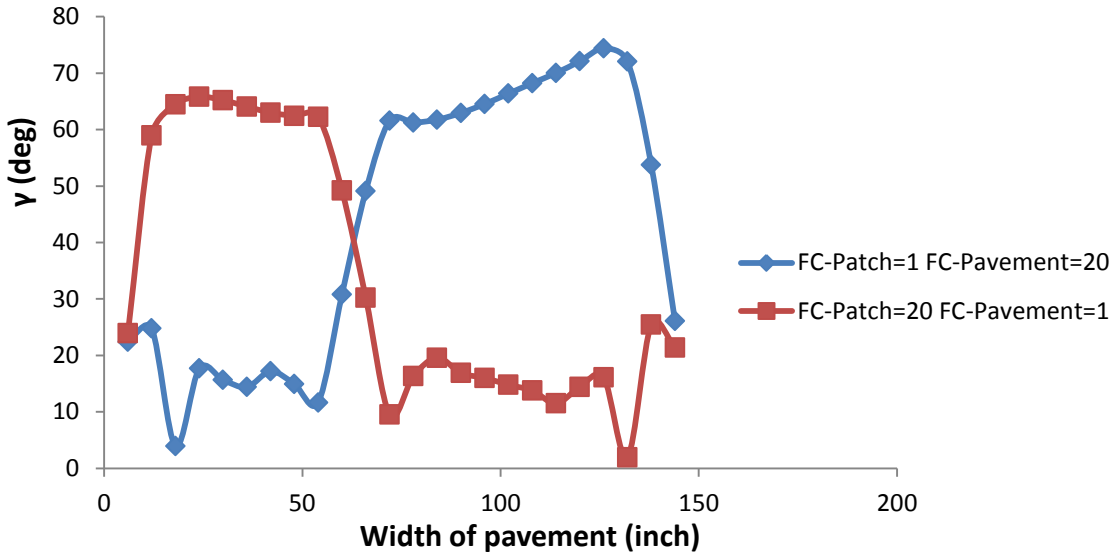

Figure 4.10 Distribution of γ along width of the pavement at transverse edge for 7' x 7' patches

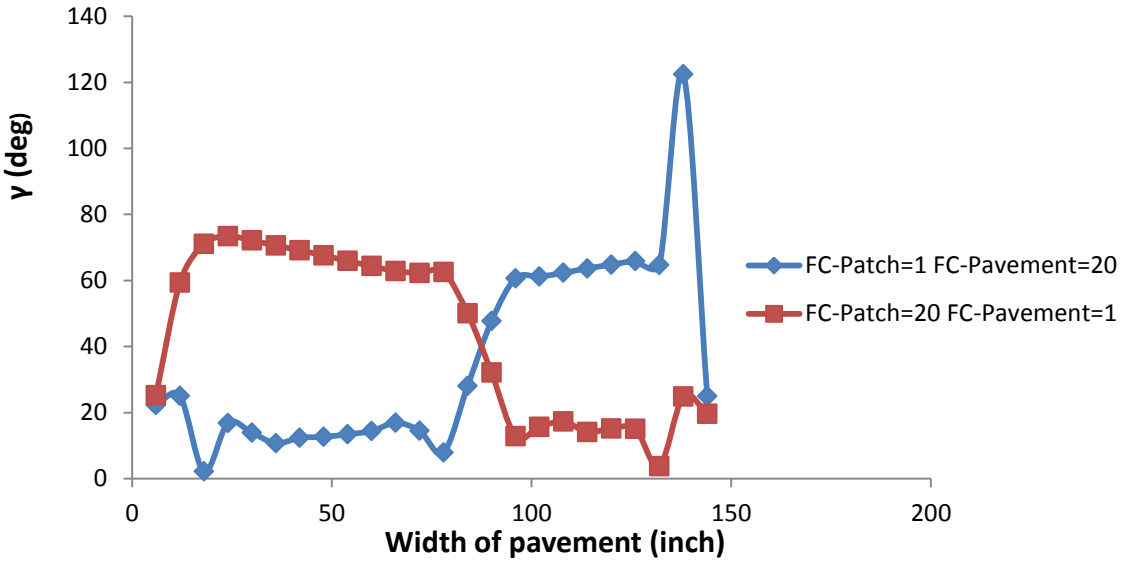

Figure 4.11 Distribution of γ along width of the pavement at transverse edge for 5' x 5' patches

4.3 Pavement with Shoulder

4.3.1 Shoulder without Joints

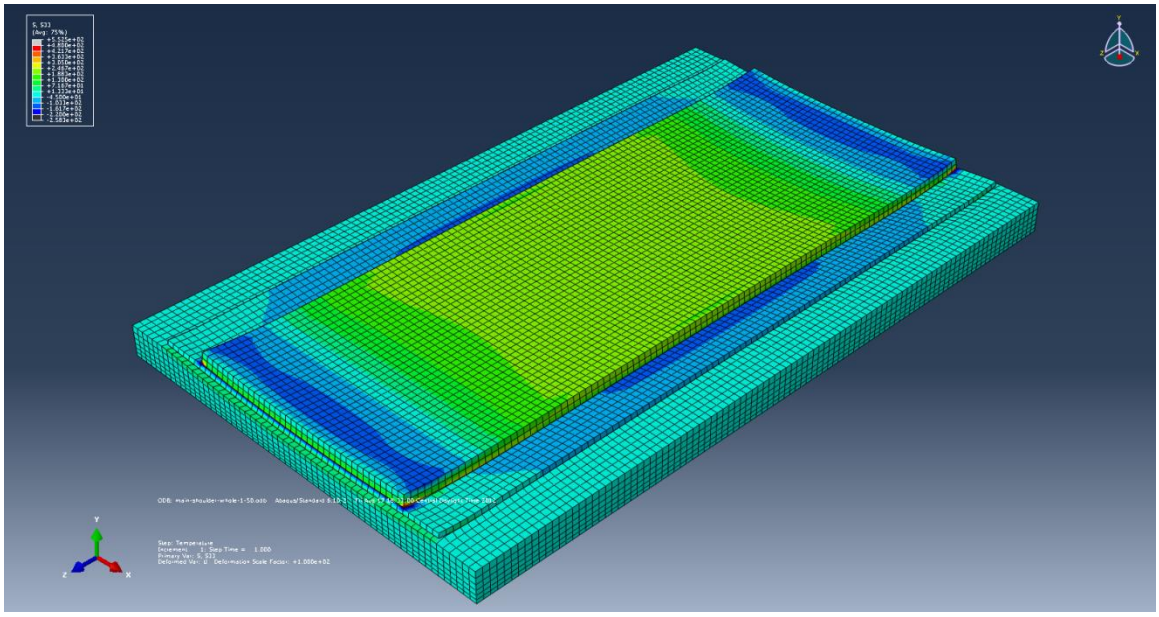

Figure 4.12 Stress map for longitudinal stresses

A color map of normal longitudinal stresses (S33) is shown in Figure 4.12. Since the pavement modeled was symmetric in the longitudinal direction, the stresses were symmetric. Figure 4.12 shows that tensile stresses developed approximately in the central areas (green areas) whereas compression stresses developed approximately at the transverse edges (blue areas) from curling of the pavement. Also, the quantity of stress in the middle of the pavement was the highest and started to decrease as it went farther from the middle. Since there was a high tensile stress in the middle, the probability of cracking in central areas was higher than transverse edges of the pavement. This also shows that the concrete pavement under ideal construction conditions will crack transverse to the pavement and not y-crack.

4.3.2 Shoulder with Joints

Figure 4.13 shows a color map of the normal longitudinal stress (S33). From Figure 4.13, it appears that when the shoulder is jointed, S33 is higher in the mainline than in the shoulder. Also, for the model with joints in the shoulder, stresses in the main line pavement were higher than stresses in the main line pavement with CRCP shoulders for the same temperature reduction in both models. As shown in Figure 4.13, there is a high concentration of stress at the sharp corners close to the joints. Also, it can be seen that stresses were not symmetric and change along the width of the pavement. This meandering in stress patterns can show a high potential for Y-cracking in the pavement with a jointed shoulder. The high stresses at the joints occur because the shoulder strains concentrate at the joint. This could lead to a situation where if the pavement cracks on the side opposite the shoulder, it would have a tendency to meander to the joint to relieve the stresses. This supports suggests that a jointed shoulder with CRCP could lead to an increase in Y-cracking.

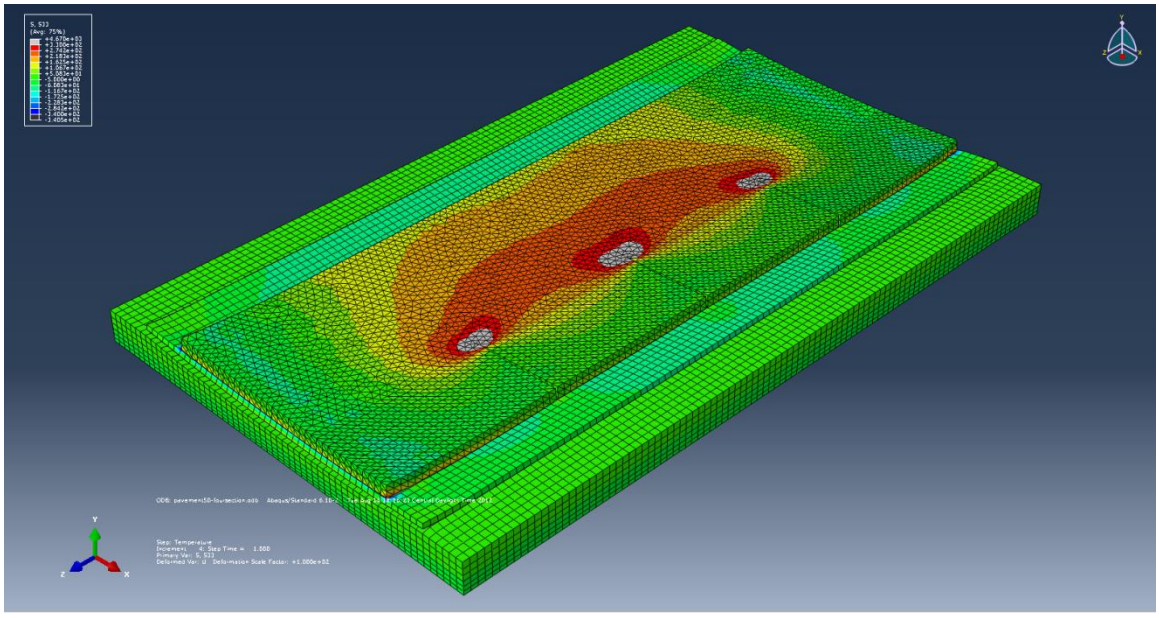

Figure 4.13 Color map for longitudinal stresses S33.

4.3.3 Different Shrinkage between Mainline and Shoulder Pavements

Directions of principal stresses were computed for the models with the 5, 10, and 40° F temperature reduction in the mainline pavement. The angle between the maximum principal stress and longitudinal axis in each element was calculated along the width of the pavement. Figure 4.14 and 4.15 show the principal stress angles at the transverse edge and in the middle of pavement, respectively. Also, Figure 4.16 and 4.17 show the orientation of these angles on 2-D plots for transverse edge and middle of the pavement respectively.

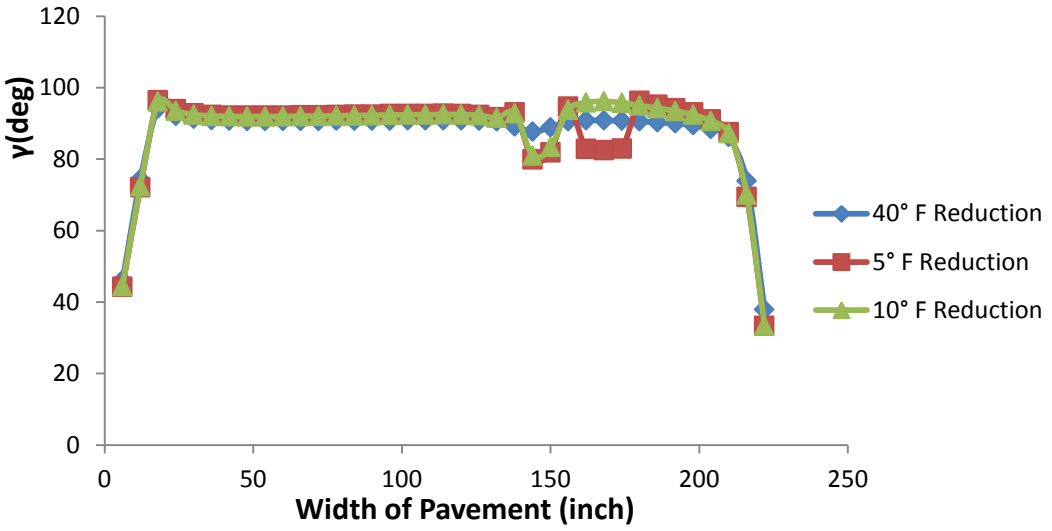

Figure 4.14 Direction of maximum principal stress for models with temperature reductions of 5°, 10° and 40° F in the mainline

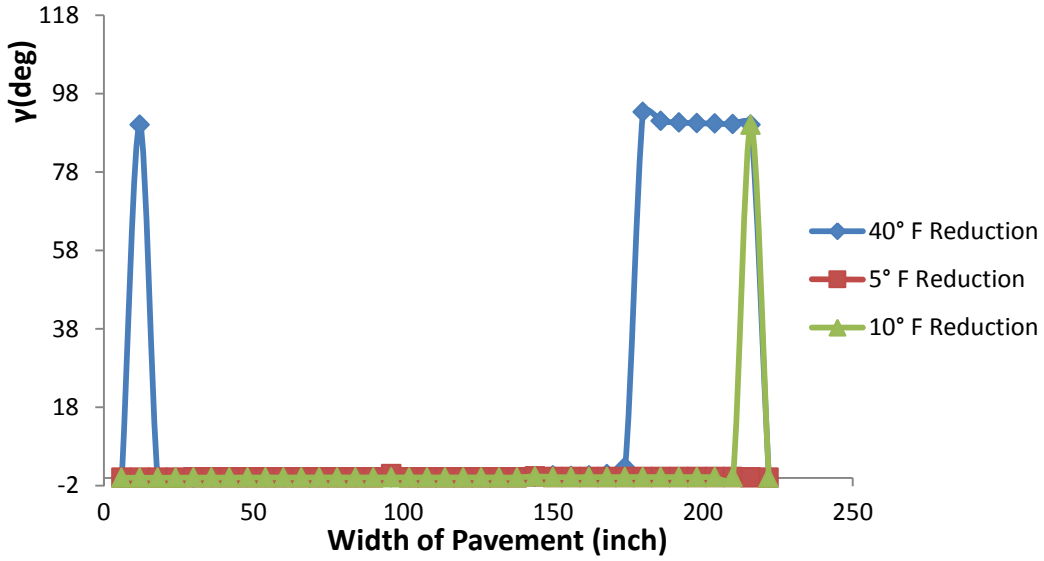

Figure 4.15 Direction of maximum principal stress for models with temperature reductions of 5°, 10° and 40° F in the mainline .

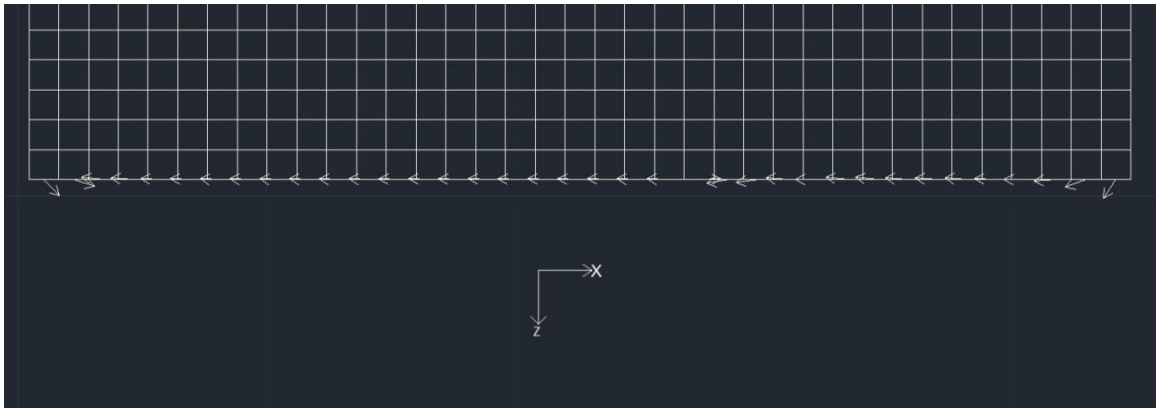

Figure 4.16 Direction of principal stress at the transverse edge of pavement for model with 10° F temperature reduction in the mainline

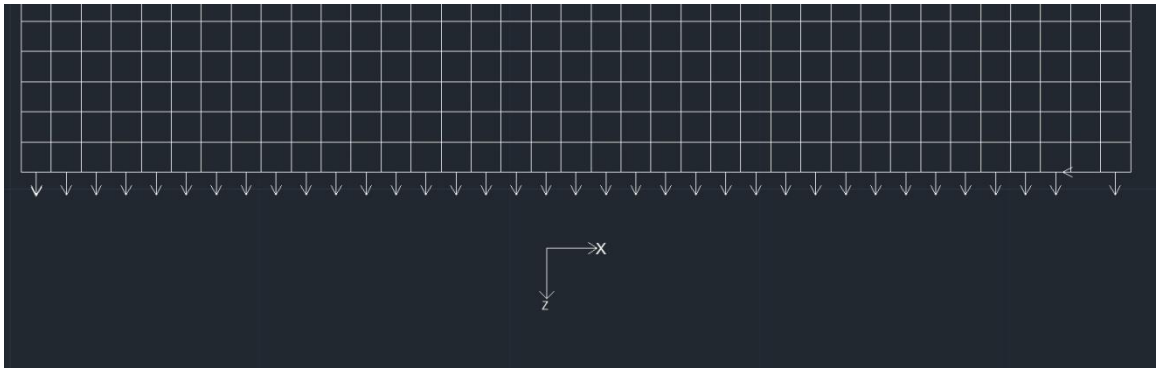

Figure 4.17 Direction of principal stress in the middle of pavement for model with 10° F temperature reduction in the mainline

From Figure 4.14, it can be seen that the orientation of the maximum principal stress was not significantly changed from different amounts of temperature decreases. Graphs in Figure 4.15 show direction of principal stress in the middle of pavement for models with temperature reductions of 5°, 10° and 40° F in mainline. It can be seen direction of principal stress for all three models was almost the same and only for model with 40° F temperature reduction there was the abrupt drop in γ from 90 degrees to 0 degrees in the right hand of width of the pavement. Principal stress angles were around 0 degree mostly along width of the pavement, which means

maximum principal stresses were almost in direction of longitudinal axis in the middle of pavement.

Figure 4.18, 4.19 and 4.20 shows respectively the color map of the normal longitudinal stresses (S33) for models with temperature reduction of 5°F, 10°F and 40°F in the mainline when the shoulder was continuously reinforced concrete pavement.

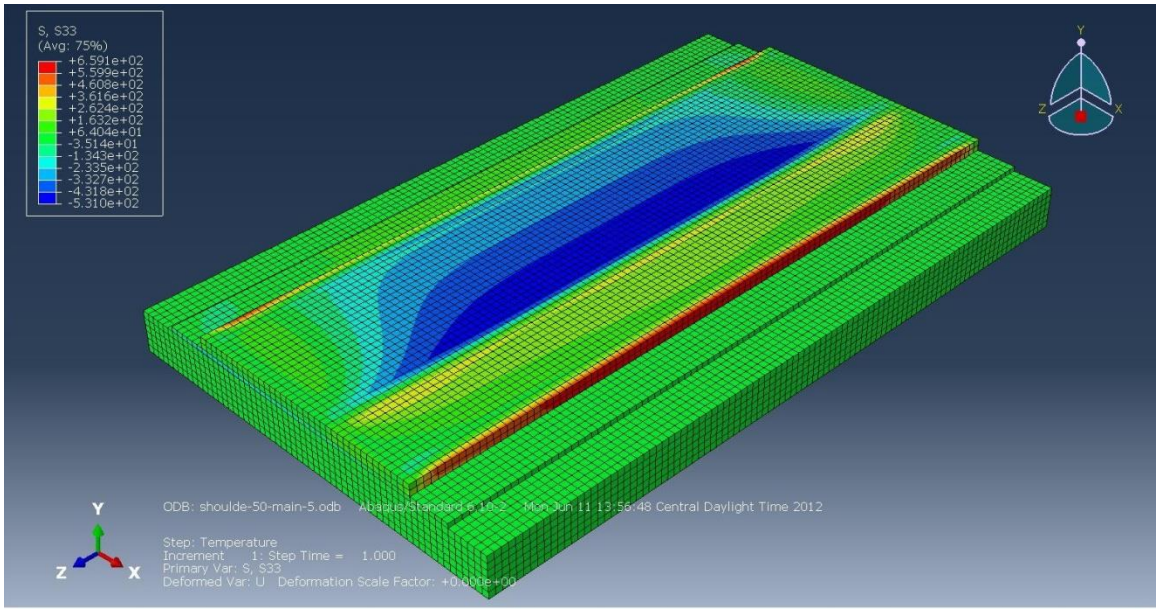

Figure 4.18 Color map of longitudinal stress (S33) for 5° F temperature reduction in the mainline for pavement with continuous shoulders

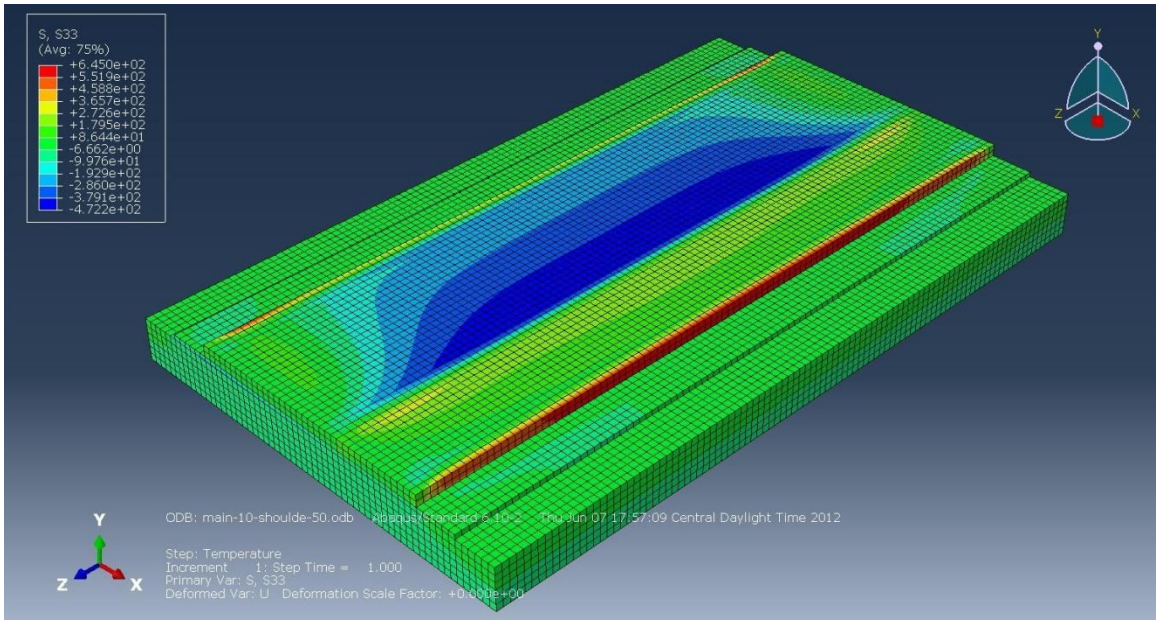

Figure 4.19 Color map of longitudinal normal stress (S33) for 10° F temperature reduction in the mainline for pavement with continuous shoulder

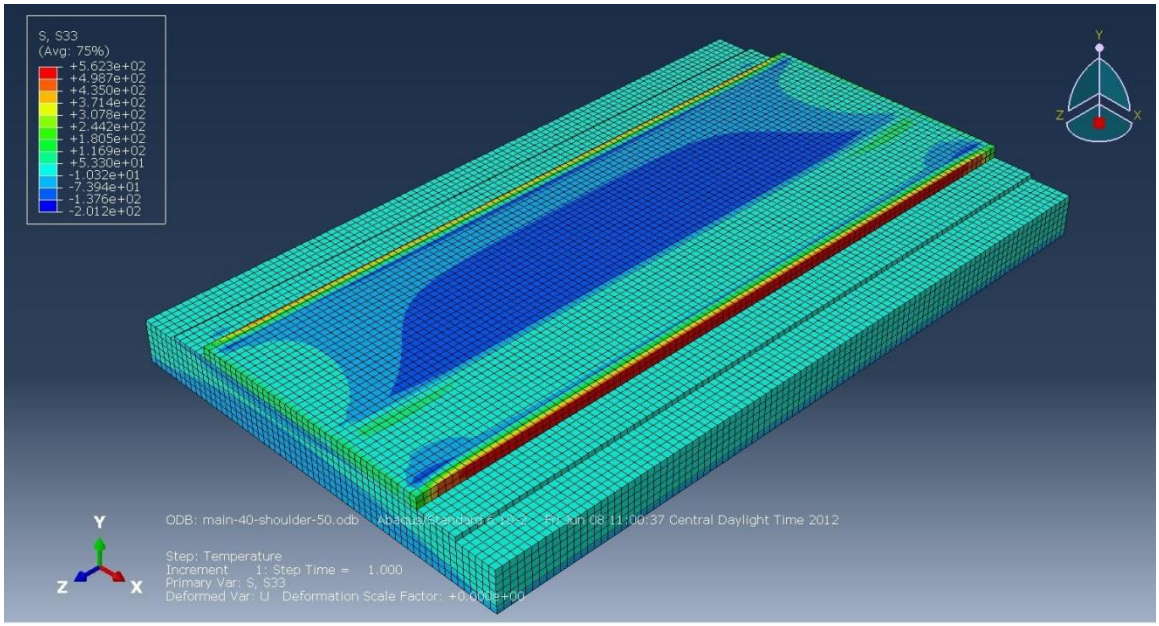

Figure 4.20 Color map of longitudinal normal stress (S33) for 40° F temperature reduction in the mainline for pavement with continuous shoulder

It can be seen from Figures 4.18, 4.19 and 4.20 that the stress magnitudes are higher for larger differences in shrinkage between the mainline and shoulder pavement. Also, there was a high tensile stress in the shoulder while the compression stress was so high in the mainline and shoulder pavement.

Another model was assembled for the pavement with jointed shoulders, but with a temperature reduction of 10°F imposed on the mainline pavement, the temperature reduction imposed on the jointed shoulder was 50°F. Figure 4.21 shows a color map of longitudinal normal stresses for this model.

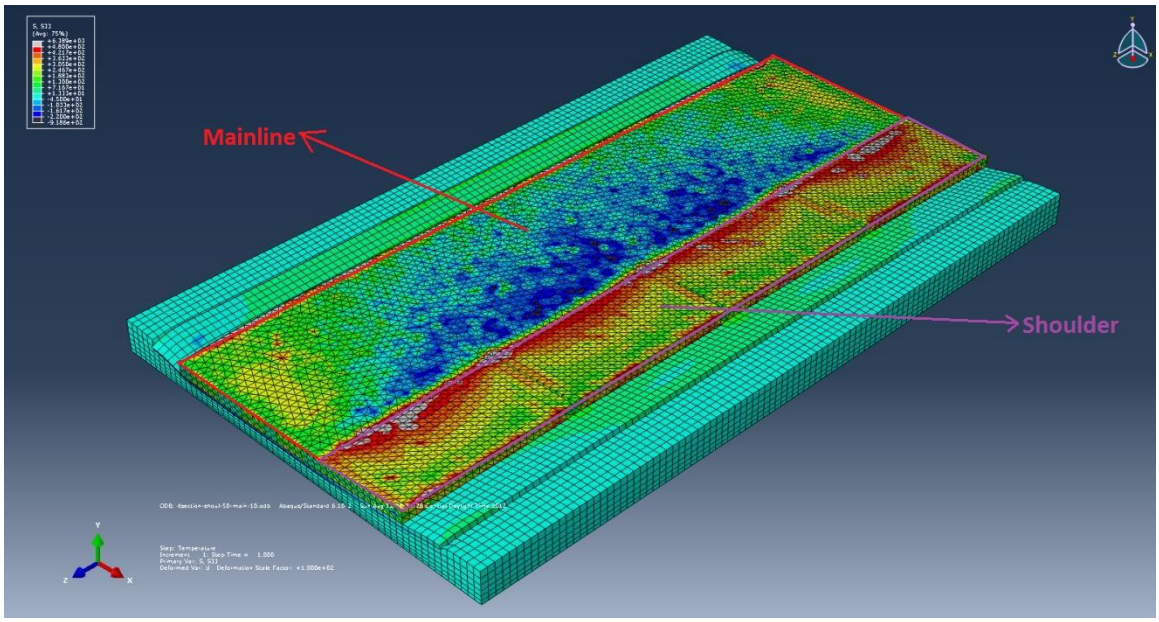

Figure 4.21 Color map of normal longitudinal stresses (S33) for pavement with jointed shoulder

From Figure 4.21, it appears that general form of stress distribution for pavements with continuous and jointed shoulder are nearly equal. However, there are high tensile stresses in the jointed shoulder, especially at the interface between the shoulder and mainline pavement (shown

in red color). Additionally, there were regions of high tensile stress in the mainline pavement at the location of the joint. Shoulder movements could concentrate at the joint, leading to high strains in the mainline pavement near the joint. This leads to high cracking potential in the mainline pavement near the shoulder joint.

4.4 Model with reinforcement

To understand the effect of reinforcement amounts on stress distribution, two finite element models with different percentages of longitudinal steel were developed.

Figure 4.22 and 4.23 show longitudinal normal stress map for model with 0.6 % and 0.7 % longitudinal steel respectively.

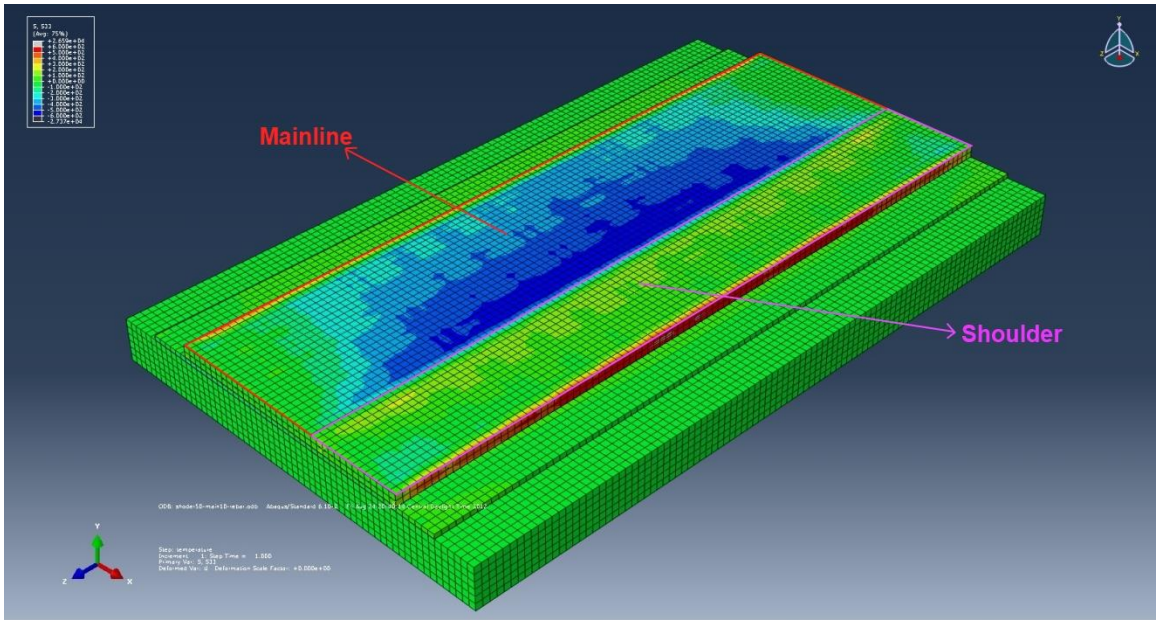

Figure 4.22 Color map of longitudinal normal stress S33 for pavement with 0.6 % longitudinal steel

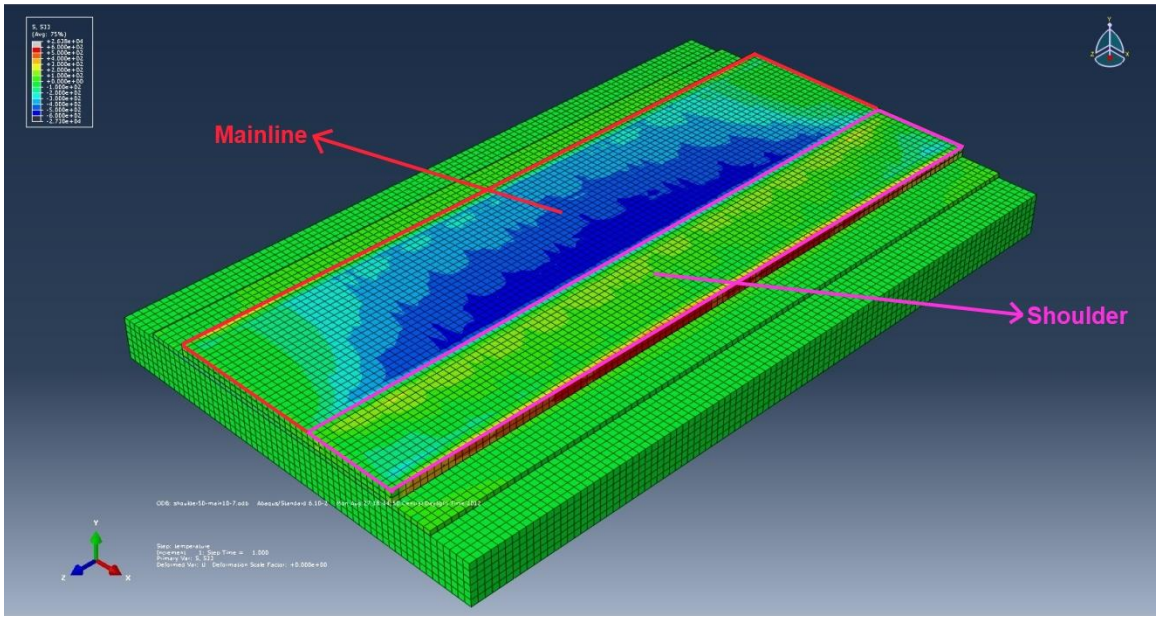

Figure 4.23 Color map of longitudinal normal stress for pavement with 0.7 % longitudinal steel

Figure 4.24 and 4.25 show normal transverse stresses (S11) map for model with 0.6 % and 0.7 % longitudinal steel respectively.

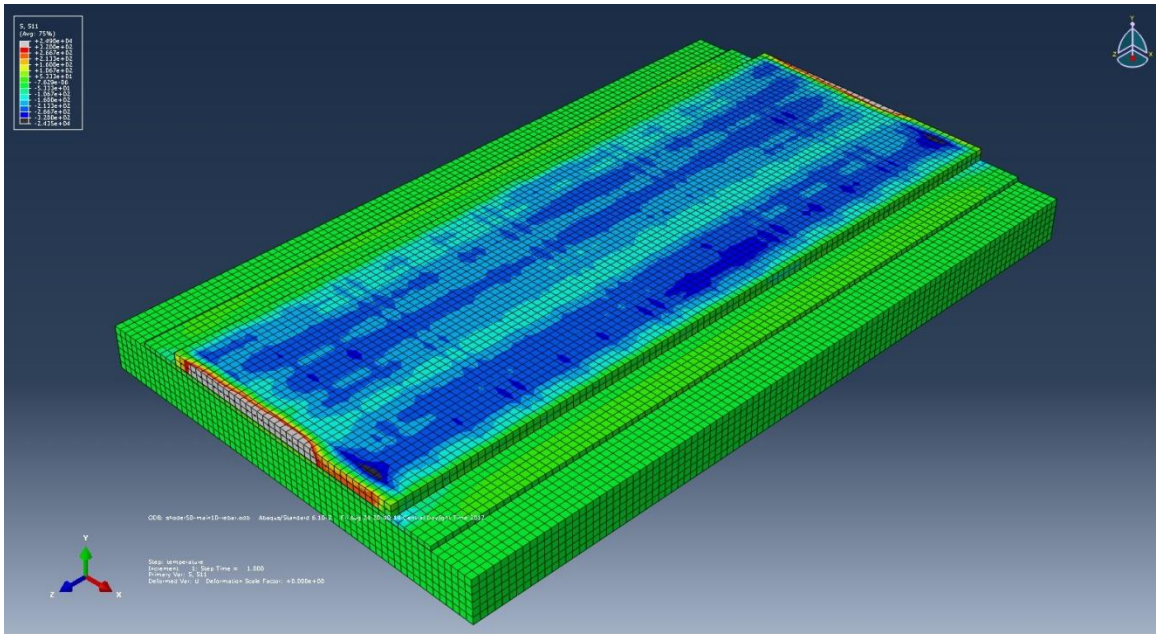

Figure 4.24 Transverse stress (S11) map for pavement with 0.6 % longitudinal steel

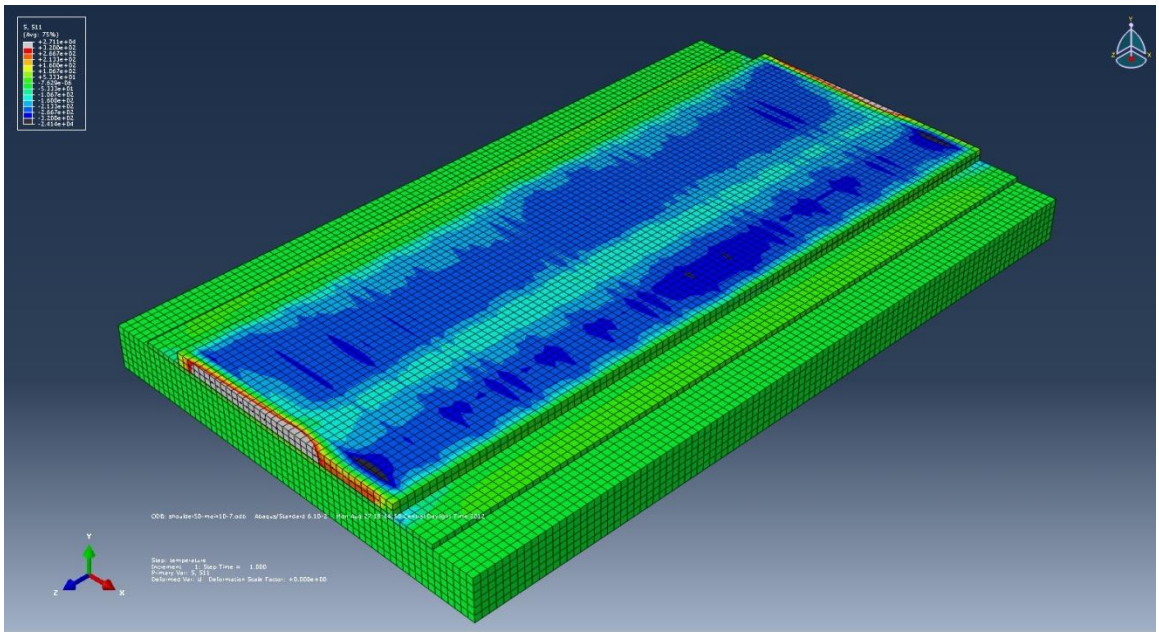

Figure 4.25 Transverse stress (S11) map for pavement with 0.7 % longitudinal steel

From Figures 4.22, 4.23, 4.24, 4.25 and after probing stress values in elements in each model, the model with 0.7% steel showed more variation in the stress, potentially leading to more crack direction diverging. Stresses in the shoulder were tensile while stresses in the mainline were predominantly compression.

Also, to see the difference in longitudinal normal stress state between reinforced and unreinforced pavement, longitudinal normal stresses were read along the width of the pavement for both models. Figure 4.26 compares S33 along the width of the pavement in the middle for unreinforced and reinforced pavement. Temp reduction in the mainline for both models was 10° F.

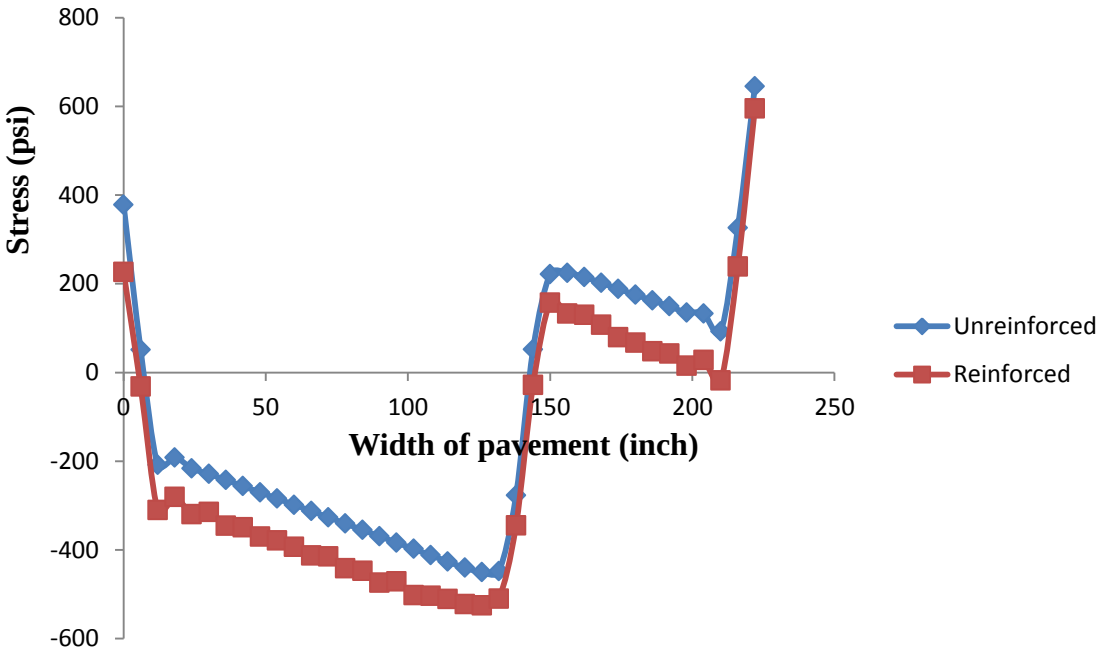

Figure 4.26 Longitudinal normal stress (S33) along the width of the pavement for reinforced and unreinforced pavement

Chapter 5 Conclusions and Recommendations

Changes in the maximum principal stress direction will cause the crack to change direction, potentially causing y-cracking. A change in the maximum principal stress along the width of the pavement also causes cracks to meander and contribute to y-cracking. In this research, several finite element simulations were run to understand the effect of friction coefficients between pavement layers, localized patch, different shrinkage between mainline and the shoulder, joints in shoulders and steel in the pavement on principal stress direction.

Models with different friction coefficients between pavement layers were developed. Different size patches with different friction coefficients were added to the pavement analysis. The impact of these patch properties on the maximum principal stress direction was studied by changing the location of patch in the pavement, patch size, and friction coefficient of interaction between patch and the underneath layer. To understand the effect of patch location, patches were placed halfway between the pavement ends in three models and in the other three models they were located at the corner. A change in the friction at the corner had a large influence on the amount of stress and direction at the edge of the patch. A patch placed midway between the pavement ends did not significantly affect the pavement stress distribution. The patch size has a large effect on the stress magnitude when the patch is near the transverse edge of the pavement or an existing crack. When the patch location is near the middle of the section between cracks in the longitudinal direction, the stresses did not change significantly. Results showed whether an increase or decrease in friction coefficient interaction will give non-uniform restraint and cause the principal stress to change direction. This data suggests that subbase non-uniformity could cause the meandering of Y-cracks.

Different temperature changes were imposed on the mainline and shoulders in order to simulate the effects of the differential drying shrinkage and temperature change between the hardened mainline concrete and the newly cast shoulder. The stress magnitudes were higher for larger differences in shrinkage between the mainline and shoulder pavement. This wavy stress patterns seen through the pavement with jointed shoulders could help explain the high potential for Y-cracking. High local stresses at the joint – mainline pavement interface could be a significant cause of y-cracking. This could lead to a situation where if the pavement cracks on the side opposite the shoulder, it would have a tendency to meander to the joint to relieve the stresses at the joint.

To understand the effect of reinforcement amounts on stress distribution, two finite element models with different percentages of longitudinal steel were developed. It appears compressive stresses are higher in model with 0.7 % longitudinal steel in comparison with model with 0.6 % steel. Also, more variation in the stress can be seen in the model with 0.7 % longitudinal steel, potentially more crack direction diverging.

It is recommended to run several models with the same properties and geometries except friction coefficients between layers in order to obtain an idea about change in stress state due to change in friction coefficients between layers. Another thing that can give researchers a good understanding of model is to experiment effects of different temperature loading on stress state in the pavement. Several models with the same properties can be run under different temperature loadings to better understand the effects of temperature loads on stress state. It is highly recommended to use fine mesh for models in order to obtain accurate results for all around the pavement. Rough meshing decreases the accuracy of results.

References

Choi, J. H., & Roger, C. H. (2005). *Design of Continuously Reinforced Concrete Pavements Using Glass Fiber Reinforced Polymer Rebars.* McLean: FHWA.

ERES Consultants, Inc. (2001). *Summary of CRCP Design and Construction Practices in the U.S.* Schaumburg, Illinois: Concrete Reinforcing Steel Institute.

Johnston, D. P., & Surdahl, R. W. (2008). Effects of Design and Material Modifications on Early Cracking of Continuously Reinforced Concrete Pavements in South Dakota. *Transportation Research Record*, 103-109.

Kohler, & Roesler. (2004). Active Crack Control for Continuously Reinforced Concrete Pavements. *Journal of the Transportation Research Board*, 19-29.

Kohler, E. E. (2006). Crack Spacing and Crack Width Investigation from Experimental CRCP Sections. *The International Journal of Pavement Engineering*, 331-340.

Kohler, E., & Roesler, J. (2006). *Accelerated Pavement Testing of Extended Life Continuously Reinforced Concrete Pavement Sections.* Springfield, IL: Illinois Department of Transportation.

McGovern, G., Ooten, D. A., & Senkowski, L. J. (1996). *Performance of Continuously Reinforced Concrete Pavements in Oklahoma.* Oklahoma City, OK: Oklahoma Department of Transportation.

Shiraz, T. D., Stephanos, P. J., Gagnon, J. S., & Zollinger, D. G. (1998). *Performance of Continiuously Reinforced Concrete Pavements Volume II-Field Investigations of CRC Pavements.* McLean: FHWA.

Suh, Y. C. (1994). Factors Affecting Crack Width of Continuously Reinforced Concrete Pavement. *Design and Rehabilitation of Pavements (Transportation Research Record)*, 134-140.

Suh, Y. C., Hankins, K., & McCullough, B. F. (1992). *Early Age Behaviour of Continuously Reinforced Concrete Pavement and Calibration of the Failure Prediction Model in the CRCP-7 Program.* Austin, TX: Texas Department of Transportation.

The Transtec Group, Inc. (2004). *CRCP inTexas Five Decades of Experience.* Schaumburg, IL: Concrete Reinforcing Steel institue.

Timm, D., Guzina, B., & Voller, V. (January 2003). Prediction of Thermal Crack Spacing. *International Journal of Solids and Structures*, 125-142.

Transportation, A. A. (1993). *AASHTO Guide for Design of Pavement Structures.* Washington, D.C.

Zollinger, D. D. (1994). Spalling of Continuously Reinforced Concrete Pavements. *Journal of Transportation Engineering*, 394-411.

Appendix A – Permissions

Yes. You have permissions as long as you make the appropriate reference. Best Regards.

-----Original Message-----
From: Amir Farid Momeni [mailto:momeni@k-state.edu]
Sent: Thursday, April 04, 2013 4:20 PM
To: Roesler, Jeffery Raphael
Subject: Figures-papers

Hello
I am Amir Farid Momeni, M.Sc student in civil engineering at Kansas State University. I worked on CRCPs and now I am writing my thesis. I was wondering if you give me permission to use figures in your paper for my thesis. These graphs are in paper titled ACCELERATED PAVEMENT TESTING OF EXTENDED LIFE CONTINUOUSLY REINFORCED CONCRETE PAVEMENT SECTIONS.
thanks

--
Graduate Research Assistant
Department of Civil Engineering
Kansas State University
2151 Fiedler Hall
Manhattan, KS 66502
momeni@ksu.edu

Dear Mr. Momeni,

Sure you can use them with the reference. I will be appreciate if you send me a copy of your paper. Thanks

2013/4/19 Amir Farid Momeni <momeni@k-state.edu>

Hello

I am Amir Farid Momeni, M.Sc student in civil engineering at Kansas State University. I worked on CRCPs and now I am writing my thesis. I was wondering if you give me permission to use figures in your paper for my thesis. These graphs are in paper titled FACTORS AFFECTING CRACK WIDTH IN CRCP.

thanks

Graduate Research Assistant
Department of Civil Engineering
Kansas State University
2151 Fiedler Hall
Manhattan, KS 66502
momeni@ksu.edu

--

Professor, Young-Chan Suh
Department of Transportation Engineering
Hanyang University,
1271 Sa-1 Dong Sangrokgu
Ansan, 425-791, Korea
(Office) +82-31-400-5155(CP) +82-10-9076-5035
suhyc@hanyang.ac.kr
http://pavement.hanyang.ac.kr/shop/index.html